QUASI-LPV MODELING AND CONTROL OF TWIN ROTOR MULTIPLE INPUT MULTIPLE OUTPUT SYSTEM

by

Halil İbrahim Baştürk

B.S, Mechanical Engineering, Boğaziçi University, 2006

Submitted to the Institute for Graduate Studies in
Science and Engineering in partial fulfillment of
the requirements for the degree of
Master of Science

Graduate Program in Mechanical Engineering
Boğaziçi University
2008

QUASI-LPV MODELING AND CONTROL OF TWIN ROTOR MULTIPLE INPUT MULTIPLE OUTPUT SYSTEM

APPROVED BY:

Assoc. Prof. İbrahim Emre Köse ....
(Thesis Supervisor)

Assist. Prof. Tankut Acarman ....

Prof. Eşref Eşkinat ....

DATE OF APPROVAL:

ACKNOWLEDGEMENTS

I would like to express my sincere gratitude to my thesis supervisor, Assoc. Prof. İbrahim Emre Köse, for his endless support in preparation of this study and for his contribution in shaping the way I do control.

I would like to thank Eşref Eşkinat and Tankut Acarman for participating in my thesis committee.

I am deeply thankful to my friends Fatih Demirkale and Elif Özer for their true friendship and motivation.

I am thankful to my officemate for a friendly atmosphere and helpful discussions Murat Güney.

Most importantly, I am indebted to my family for their self-sacrifice and patience through my education.

ABSTRACT

QUASI-LPV MODELING AND CONTROL OF TWIN ROTOR MULTIPLE INPUT MULTIPLE OUTPUT SYSTEM

The aim of this thesis is to design a Linear Parameter Varying (LPV) controller for Twin Rotor Multiple Input Multiple Output System (TRMS) which has highly nonlinear and cross coupled mathematical model, using Linear Matrix Inequalities (LMIs). The *quasi*-LPV model of TRMS is written by considering the nonlinearities in the mathematical model as time varying parameters. In this way, Linear Fractional Transformation (LFT) form of the model is obtained. LMI condition for the existence of the controller and stability of the desired closed loop system are developed as indicated in the literature using the LFT form of the model. Developed LMIs conditions are solved for decision variables and the LPV controller for TRMS is obtained.

The simulation is performed for different modes. In results, it is seen that simulation of the LPV controller with the nonlinear TRMS yields excellent results for different modes, in spite of nonlinearity and cross coupling in the model.

ÖZET

SANKİ-DPD MODELLEMESİ VE İKİZ MOTORLU ÇOK GİRDİLİ ÇOK ÇIKTILI SİSTEM KONTROLÜ

Bu tezin amacı, Doğrusal Matris Eşitsizliklerini (DME) çözerek, çapraz ilişkili doğrusal olmayan matematiksel modele sahip İkiz Motorlu Çok Girdili Çok Çıktılı Sistem (İMÇS) için Doğrusal Parametre Değişeni (DPD) kontrolcüsü tasarlamaktır. Sistemin matematiksel modelinde doğrusal olmayan terimleri zamanla değişen parametreler olarak kabul ederek, sistemin *sanki*-(DPD) modeli yazıldı. Böylelikle, modelin Doğrusal Kesirli Dönüşüm (DKD) formu elde edildi. Bu form kullanılarak, kontrolcünün varolma durumu ve kapalısistemin dengede olma durumu literatürde belirtildiği gibi DME cinsinden oluşturuldu. Oluşturulan DME karar verilecek değişkenler için çözülerek DPD kontrolcüsü elde edildi.

Farklı durumlar icin similasyon yapıldı. Sonuçlarda şu görüldü ki, modeldeki çapraz ilişkili ve doğrusal olmayan terimlere rağmen, İMÇS doğrusal olmayan modeli DDP kontrolcüsüyle farklı durumlar için similasyonda mükemmel sonuçlar verdi.

TABLE OF CONTENTS

LIST OF FIGURES

LIST OF TABLES

LIST OF SYMBOLS/ABBREVIATIONS

a_v	Pitch angle of the system
a_h	Yaw angle of the system
$\underline{F}_{h/v}$	Aerodynamic force from the tail/main rotor
$\underline{g}$	Gravitational acceleration
$K_{v/h}$	Voltage constant of the main/tail D.C. motor
k_{fv}	Friction constant for vertical axis
k_{fh}	Friction constant for horizontal axis
k_{pv}	Aerodynamic force constant for main rotor
k_{ph}	Aerodynamic force constant for tail rotor
l_t	Length of the tail part of the beam
l_b	Length of counterweight beam
l_{cb}	Distance between counterweight and the joint
l_m	Length of the main part of the beam
m_b	Mass of the counterweight beam
m_{cb}	Mass of counterweight
m_m	Mass of the main part of the beam
m_{mr}	Mass of the main D.C motor
m_{ms}	Mass of the main shield
m_t	Mass of the tail part of the beam
m_{tr}	Mass of the ail D.C motor
m_{ts}	Mass of the tail shield
$\underline{M}_{fric,v}$	Moment of the friction force for vertical axis
$\underline{M}_{fric,h}$	Moment of the friction force for horizontal axis
r_{ms}	Radius of the main shield
r_{ts}	Radius of the tail shield
$\underline{S}_h$	Angular momentum in the horizontal plane
$\underline{S}_v$	Angular momentum in the vertical plane
$T_{v/h}$	Angular constant of the main/tail D.C. motor
$\underline{w}_h$	Angular velocity of the tail rotor

$\underline{w}_v$	Angular velocity of the main rotor
TRMS	Twin Rotor Multiple Input Multiple Output System

1. INTRODUCTION

1.1. Twin Rotor Multiple Input Multiple Output System

Twin Rotor Multiple Input Multiple Output System (TRMS) is a laboratory set-up which is developed by Feedback Instruments Limited for control experiments.

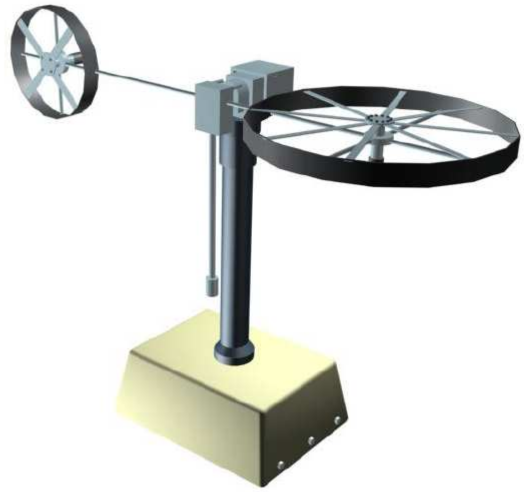

Figure 1.1. Overview of TRMS

TRMS, as shown on the Figure 1.1 [1], has two propellers which are driven by d.c. motors. Propellers are joined by beam and they are perpendicular to each other. Joined beam can rotate freely in the horizontal and vertical planes by changing the input voltage of the d.c motors. Pendulum counterweight hanging from the beam is used to balance the system in steady state.

With highly non-linear dynamics and cross coupling between its two axes, TRMS is one of the challenging engineering problem. It is similar to a real helicopter in some ways. For example, it has a strong cross coupling between main and tail rotor, as helicopter. However, TRMS and helicopter have many differences. The main differences are listed on the Table 1.1 [1].

Table 1.1. Main Differences Between TRMS and Helicopter

Properties	TRMS	Helicopter
Location of pivot point	Midway between two rotors	Main rotor head
Vertical control	Speed control of main rotor	Pitch angle of main rotor blades
Horizontal control	Speed control of tail rotor	Pitch angle of tail rotor blades

1.1.1. TRMS Mechanical Unit Description

The Mechanical Unit of the TRMS (except the base and the tower) consists of the following elements:

- Main Rotor -enables vertical thrust control
- Tail Rotor -enables horizontal thrust control
- Counter Balance -counter weight for the main rotor

The figure 1.2 [1] illustrates the Mechanical Unit of the TRMS

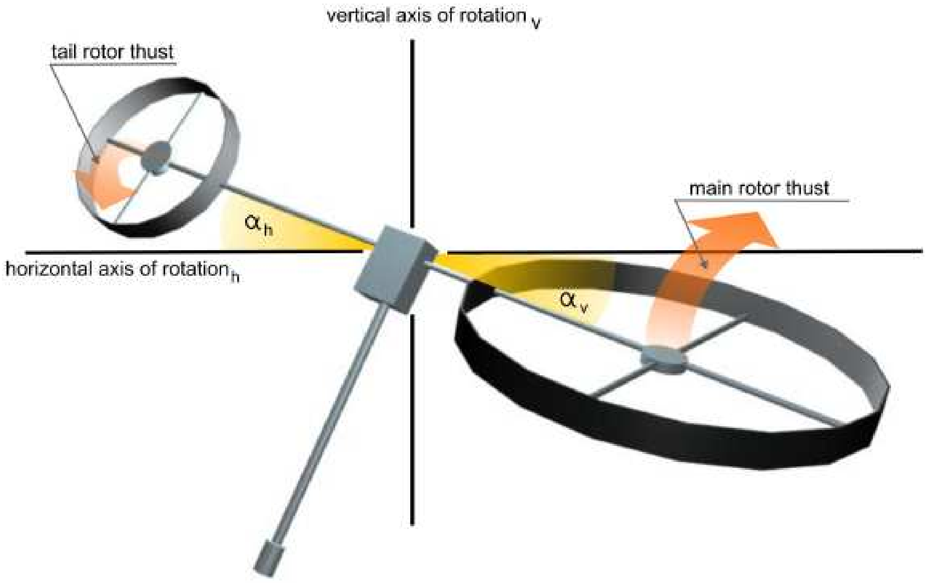
vertical axis of rotation $_v$
tail rotor thust
main rotor thust
α_h
horizontal axis of rotation $_h$
α_v

Figure 1.2. Mechanical Unit of TRMS

1.1.2. TRMS Electrical Unit Description

Apart from mechanical units, the electrical unit plays an important role for TRMS control. It allows to transfer the measured signals to the PC and control signal application. The system consist of three main elements:

- PC with a clocked control algorithm
- $A \setminus D$ and $D \setminus A$ converters - serving as an interface between the PC and external environment
- Encoders

The encoders measure the relative position. This is an important point to be taken into consideration in the TRMS applications.

The control system diagram is illustrated in figure 1.3 [1].

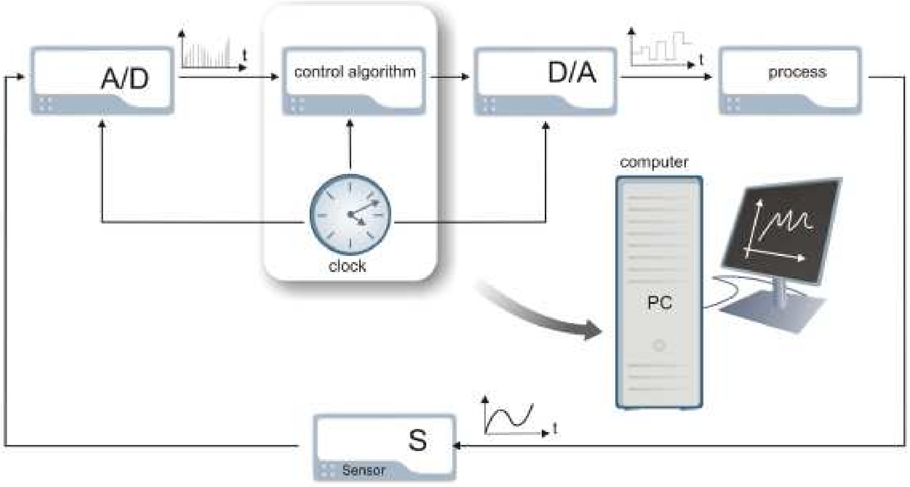

Figure 1.3. Control System Diagram

1.2. Linear Matrix Inequalities (LMIs)

The analysis of the system and the synthesis of the controller discussed in this thesis are based on the Linear Matrix Inequalities (LMIs). Firstly, the sign definiteness of the matrices should be considered to express the LMIs. The sign definiteness of the matrices are not expressed as the same for scalar values.

A matrix $A = A^T \in R^{n\times n}$ is said to be [10]

- Positive Definite if $x^TAx > 0$, $\forall x \in R^n$, $x \neq 0$
- Negative Definite if $x^TAx < 0$, $\forall x \in R^n$, $x \neq 0$
- Positive Semi-Definite if $x^TAx \geq 0$, $\forall x \in R^n$, $x \neq 0$
- Negative Semi-Definite if $x^TAx \leq 0$, $\forall x \in R^n$, $x \neq 0$

The sign definiteness can be also expressed by the eigenvalue(λ) of the matrix. A matrix $A = A^T \in R^{n\times n}$ is said to be [10]

- Positive Definite if and only if $\lambda_i > 0$, $\forall i = 1 : n$
- Negative Definite if and only if $\lambda_i < 0$, $\forall i = 1 : n$
- Positive Semi-Definite if and only if $\lambda_i \geq 0$, $\forall i = 1 : n$
- Negative Semi-Definite if and only if $\lambda_i \leq 0$, $\forall i = 1 : n$

From now on, we will use the symbols $\succ, \succeq, \prec, \preceq$ to express the sign of a matrix.

Consider the real symmetric matrices $F_0, \cdots, F_m \in R^{n\times n}$ and the decision variables $x_1, \cdots, x_m \in R^n$. A linear matrix inequality is an expression of the form [7]

$$F(x) := F_0 + x_1F_1 + \cdots + x_mF_m \succ 0$$

The set of finite linear matrix inequalities can be expressed as a system of linear matrix inequalities in one inequality.

$$F_1(x) > 0, \cdots, F_k(x) \succ 0$$

can be expressed as [7]

$$F(x) := \begin{pmatrix} F_1(x) & 0 & \dots & 0 \\ 0 & F_2(x) & \dots & 0 \\ \vdots & \vdots & \ddots & \vdots \\ 0 & 0 & \dots & F_k(x) \end{pmatrix} \succ 0$$

This property is very useful to express and solve the LMIs in a simple way.

The linear matrix inequalities in dynamical systems and control begin with the doctoral dissertation of Aleksandr Mikhailovich Lyapunov in 1892 [7]. When this idea is applied to an autonomous system $\dot{x} = Ax$, one can say that this system is asymptotically stable if and only if there exists an $X = X^T$ such that the LMI condition

$$\begin{pmatrix} X & 0 \\ 0 & -A^T X - XA \end{pmatrix} \succ 0$$

is satisfied. The use of LMIs in control theory is generally based on this idea. For many more applications, see [6].

At the present time, the LMIs can be developed on the computer and obtained the solutions easily by the MATLAB-based solvers and toolbox. In this thesis, we use YALMIP toolbox to define the LMIs and SeDuMi as solver. The usage procedure of toolbox and solver are discussed in detail in the Chapter 5.

1.3. Problem Statement

The control of the TRMS has been studied with different methods. The dynamic modeling and optimal control of TRMS is presented in reference [2]. Performance analysis of four types of conjugate gradient algorithm in the non-linear dynamic modeling of TRMS using feedforward neural networks has been reported in reference [3]. Aldebrez *et al.* [4] have proposed the parametric modeling of TRMS using a genetic algorithm.

In this thesis, we have investigated the use of linear parameter-varying (LPV) controller design for the TRMS. The non-linearities in the mathematical model of the TRMS are considered as time varying parameters. In this way, the a linear fractional transformation (LFT) form of the dynamical model of the TRMS is obtained. It is well-known that the stability conditions for uncontrolled parameter-dependent systems can be expressed in terms of LMIs [7]. For systems with control inputs and measured outputs, stabilizing controllers can be obtained using the stability conditions for the closed-loop system. Indeed, the resulting existence conditions for such controllers constitute LMI conditions as well.

The thesis is organized as follows: In Chapter 2, nonlinear mathematical and *quasi*-LPV model of the TRMS is derived. The discussion about the LPV systems and LFT connection is given in Chapter 3. In Chapter 4, LPV controller design is discussed. Application of the theory to TRMS and simulation procedure are given in Chapter 5. The results of simulation for different modes are presented in Chapter 6. Final discussion are mentioned in Conclusion part.

2. Modeling of the TRMS

In this chapter non-linear model of the TRMS will be discussed. There are two important approaches to model a dynamic system; ”Newtonian” and ”Lagrangian”. In reference [5], the two approaches for TRMS have been discussed. In this thesis, Newtonian based model of the TRMS has been discussed.

2.1. Nonlinear Model of the TRMS

The modeling of the TRMS is based on the newtonian approach. The derivative of the angular momentum of the system with respect to time equals to sum of the moments that affect the system. This idea can be shown as

$$\underline{M}_{O_{total}} = \underline{\dot{H}}_{O_{body}} + \underline{\omega} \times \underline{H}_{O}, \tag{2.1}$$

where

$\underline{M}_{total}$: total moment about point O, $\underline{H}_{O}$: angular momentum about point O,
$\underline{\omega}$: angular velocity of the body frame, $\underline{\dot{H}}_{O_{body}}$: $\underline{\dot{H}}_{O}$ as observed from the body frame

The vertical and horizontal free body diagram of the TRMS can be illustrated in Figures 2.1 [5] and 2.3 [5]. Because of the propellers, there is cross coupling in the system. TRMS can be simplified by ignoring propellers as indicated in Figures 2.2 and 2.4. Affects of the propellers to the system will be added by empirical term at the end of the each sections. Consider the dimensions, masses and propellers forces remain same.

2.1.1. Mathematical Model of Vertical Axis

The modeling idea based on the equation (2.1). If the body frame is placed on the point O and the moment of inertia of the system and the total moment of the system are calculated with respect to point O, the second term of the (2.1) became zero. The

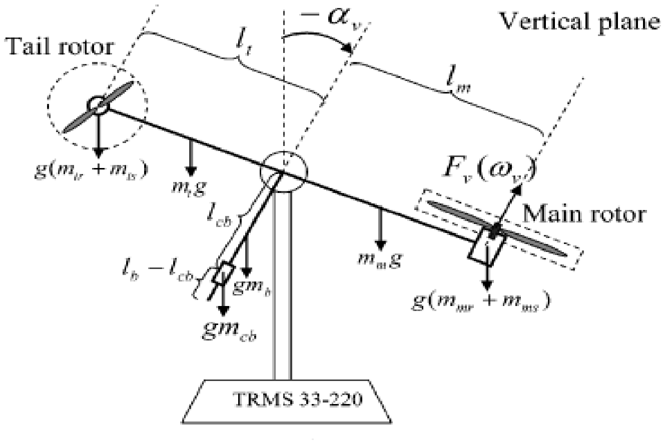

Figure 2.1. The Free-body Diagram of Vertical Axis

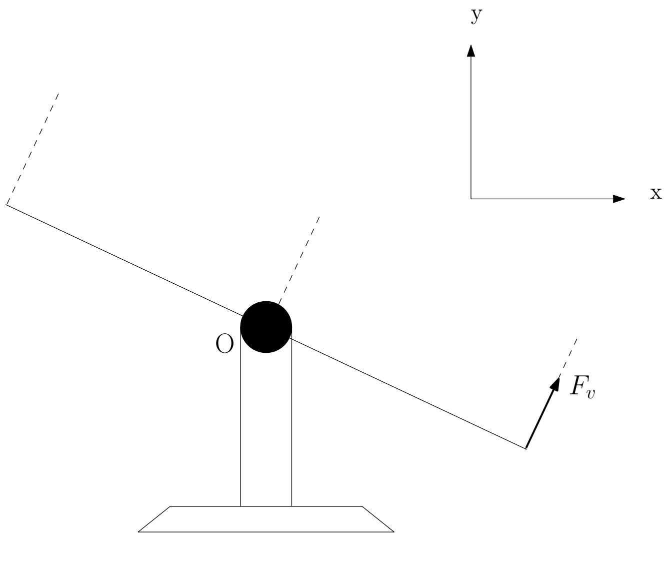

Figure 2.2. Simplified Model (Vertical)

calculation of the moment of inertia about horizontal axis is presented in Appendix A. This way, we obtained the following equation for vertical axis,

$$\begin{aligned} \underline{M}_{Ov_{total}} &= \frac{d\underline{S}_v}{dt} & \underline{S}_v &:= \text{Angular momentum in vertical plane} \\ &= J_{Ov}\frac{d\dot{a}_v}{dt} & J_{Ov} &:= \text{Moment of inertia about horizontal axis} \end{aligned} \tag{2.2}$$

The terms that affects the moment of vertical axis can be summarized as

- Propulsive Force
- Friction Moment
- Gravity Force
- Centrifugal Force

In references [5] and [1], the propulsive force and friction moment are given as

$$\underline{F}_{v/h}(\underline{w}_{v/h}) = k_{pv/h}\,\mathrm{sgn}(\underline{w}_{v/h})\underline{w}_{v/h}^2 \tag{2.3}$$

$$\underline{M}_{fric,v/h} = k_{fv/h}\underline{\dot{a}}_{v/h} \tag{2.4}$$

The total moment of the vertical axis ($\underline{M}_{v_{total}}$) can be written as

$$\begin{aligned} \frac{d\underline{S}_v}{dt} &= \underline{M}_{v_{total}} \\ &= l_m\underline{F}_v(\underline{w}_v) - \underline{M}_{fric,v} + \underline{g}[(A-B)\cos(a_v) - C\sin(a_v)] - 0.5\underline{\dot{a}_h}^2 H\sin(2a_v) \end{aligned} \tag{2.5}$$

where

$$A := (m_t/2 + m_{tr} + m_{ts})l_t, \tag{2.6a}$$

$$B := (m_m/2 + m_{mr} + m_{ms})l_m, \tag{2.6b}$$

$$C := (m_b l_b/2 + m_{cb} l_{cb}) \tag{2.6c}$$

$$H := Al_t + Bl_m + m_b l_b^2/2 + m_{cb} l_{cb}^2. \tag{2.6d}$$

The angular velocity of the vertical axis can be written

$$\underline{S}_v = J_v \underline{\dot{a}}_v \tag{2.7}$$

$$\Longrightarrow \underline{\dot{a}}_v = \frac{\underline{S}_v}{J_v} \tag{2.8}$$

So far in the model, we did not take the propellers into consideration. However, they are the main part of the cross coupling of the system. This affect is given by term $\frac{k_t w_h}{J_v}$ as indicated in references [5] and [1]. When we add the affect of the empirical term to the system. The final equation becomes as follow

$$\underline{\dot{a}}_v = \frac{d\underline{a}_v}{dt} \tag{2.9}$$

$$= \frac{\underline{S}_v}{J_v} + \underbrace{\frac{k_t \underline{w}_h}{J_v}}_{\text{effect of the tail propeller on vertical axis movement}} \tag{2.10}$$

2.1.2. Mathematical Model of Horizontal Axis

The idea used for vertical axis is same for horizontal axis. Because the second term of the equation (2.1) is zero for our situation. The calculation of the moment of inertia about vertical axis is presented in Appendix A. The following expression can be written for horizontal axis

$$\underline{M}_{Oh_{total}} = \frac{d\underline{S}_h}{dt} \qquad \underline{S}_v := \text{Angular momentum in horizontal plane}$$

$$= J_{Oh}\frac{d\dot{a}_h}{dt} \qquad J_{Oh} := \text{Moment of inertia about vertical axis axis} \tag{2.11}$$

As it can be considered from Figure 2.3, the terms that affect the moment of the horizontal axis are

- Propulsive Force
- Friction Moment

The total moment of the horizontal axis $\underline{M}_{h_{total}}$ can be written as

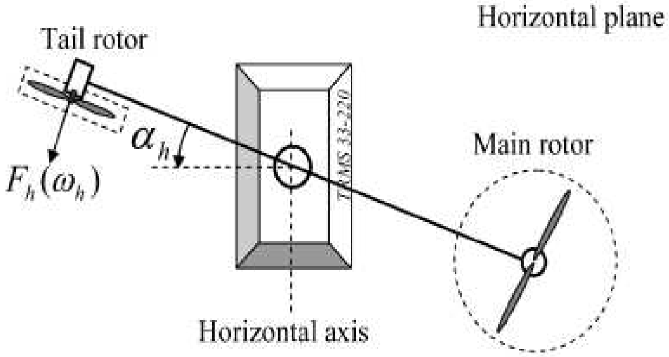

Figure 2.3. The Free-body Diagram of Vertical Axis

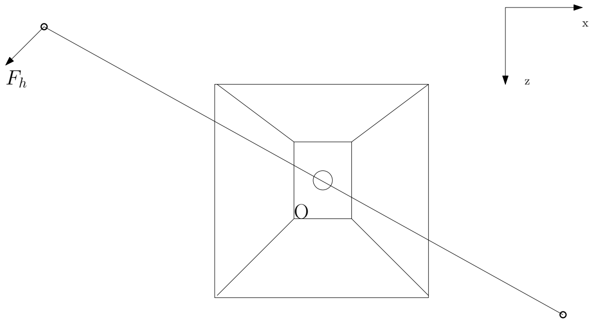

Figure 2.4. Simplified Model (Horizontal)

$$\frac{d\underline{S}_h}{dt} = \underline{M}_{h_{total}} \tag{2.12}$$

$$= l_t\underline{F}_h(w_h) - \underline{M}_{fric,h} \tag{2.13}$$

The angular velocity of the horizontal axis can be written as

$$\underline{S}_h = J_h\dot{\underline{a}}_h \tag{2.14}$$

$$\Longrightarrow \dot{\underline{a}}_h = \frac{\underline{S}_h}{J_h} \tag{2.15}$$

So far in the model, we did not take the propellers into consideration. However, they are the main part of the cross coupling of the system. This affect is given by term $\frac{k_t\underline{w}_v\cos(a_v)}{J_h}$ as

[5] and [1]. When we add the affect of the empirical term to the system. The final equation becomes as follows

$$\underline{\dot{a}}_h = \frac{d\underline{a}_h}{dt} \tag{2.16}$$

$$= \frac{\underline{S}_h}{J_h} + \underbrace{\frac{k_m \underline{w}_v \cos(a_v)}{J_h}}_{\text{effect of the main propeller on horizontal axis movement}} \tag{2.17}$$

2.1.3. Mathematical Model of DC Motor

The inputs of the overall TRMS system are voltages to the main and the tail propeller DC motors and the outputs are the pitch and the yaw angles. The DC motors convert input voltage to the angular velocity at their output shafts and thus activate the propellers (A simplified circuit diagram for a DC motor is illustrated in figure 2.5). In this section, the relationship between input voltage and angular velocity is described.

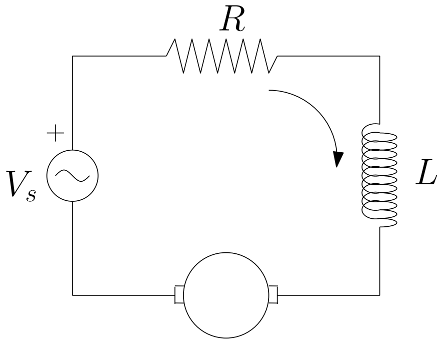

Figure 2.5. The Circuit Diagram of D.C. Motor

The following equation can be derived by applying Kirchhoff's law to the circuit shown in Figure 2.5

$$V - V_R - V_L - V_n = 0, \tag{2.18}$$

where

$$V_r := Ri \tag{2.19}$$

$$V_l := L\frac{di}{dt} \tag{2.20}$$

$$V_n := k_n w. \tag{2.21}$$

Substituting equations (2.19), (2.20) and (2.21) into equation (2.18) gives the following equation [13]

$$V - Ri - L\frac{di}{dt} - k_n w = 0. \tag{2.22}$$

The following equation can be derived by applying Newton's law to the circuit shown in Figure 2.5

$$T_e - T_{w'} - T_w - T_L = 0 \tag{2.23}$$

$$T_e := k_r i \tag{2.24}$$

$$T_{w'} := J\frac{dw}{dt} \tag{2.25}$$

$$T_w := Bw \tag{2.26}$$

$$T_L := B_L w_L, \tag{2.27}$$

where T_e is the electromagnetic torque, $T_{w'}$ is the torque due to rotational acceleration of the rotor, T_w is the torque produced from the velocity of the rotor, and T_L is the torque of the mechanical load.

Substituting equations (2.24), (2.25), (2.26) and (2.27) into equation (2.23) gives the following equation [13]

$$k_r i - J\frac{dw}{dt} - Bw - B_L w_L = 0. \tag{2.28}$$

When the system reaches steady state, the time derivative of the current ($\frac{di}{dt} = 0$) equals to zero. For the propeller, it can be assumed that $w = k_L w_L$. With these assumptions, the combination of equations (2.22) and (2.28) by eliminating the current i, gives the following equation

$$\frac{dw}{dt} = -\frac{k_r}{JR}\left[\frac{R(B+B_L k_L)}{k_r} - k_n\right] w + \frac{k_r}{JR} V \tag{2.29}$$

Define $\frac{k_r}{JR}\left[\frac{R(B+B_L k_L)}{k_r} - k_n\right] = \frac{1}{T}$ and $\frac{k_r}{JR} = \frac{1}{K}$. In this way, equation (2.29) can be rewritten as

$$\frac{d}{dt} w_{v/h} = -\frac{1}{T_{v/h}} w_{v/h} + \frac{1}{K_{v/h}} u_{v/h} \tag{2.30}$$

2.2. Quasi-LPV Modeling of the TRMS

In the previous chapter, the nonlinear mathematical model of the TRMS was obtained. If we treat the nonlinear terms in the model as time-varying parameters, we can use the available results in the LPV control literature. Such a model, *i.e.,* one where nonlinear terms involving the state variables are treated as time-varying parameters, is referred to as a *quasi-LPV* model. To obtain a quasi-LPV model of the TRMS, the state-space representation of the model must first be derived.

The time derivative of equations (2.14) and (2.16) can be written as

$$\ddot{a}_v = \frac{1}{J_v}\frac{dS_v}{dt} + \frac{k_t}{J_v}\frac{dw_h}{dt} \tag{2.31}$$

and

$$\ddot{a}_h = \frac{1}{J_h}\frac{dS_h}{dt} + \frac{k_m}{J_h}\frac{d(w_v \cos(a_v))}{dt}. \tag{2.32}$$

Although the moment of inertia along the vertical axis, namely J_h, depends on a_v nonlinearly, it is taken as constant.

Substituting equations (2.5), (2.12) and (2.30) into equations (2.31) and (2.32) respectively, gives following equations

$$\ddot{a}_v = \frac{1}{J_v}[l_m F_v(w_v) - M_{fric,v} + g[(A-B)\cos(a_v) - C\sin(a_v)] \\ - 0.5\dot{a}_h^2 H \sin(2a_v)] + \frac{k_t}{J_v}\left(-\frac{1}{T_h}w_h + \frac{1}{K_h}u_h\right) \tag{2.33}$$

$$\ddot{a}_h = \frac{1}{J_h}(l_t F_h(w_h) - M_{fric,h}) - \frac{k_m w_v \sin(a_v)\dot{a}_v}{J_h} + \frac{k_m \cos(a_v)}{J_h}(-\frac{1}{T_v}w_v + \frac{1}{K_v}u_v) \tag{2.34}$$

The states and the control inputs can be chosen as

$$x = \begin{pmatrix} a_v \\ \dot{a}_v \\ a_h \\ \dot{a}_h \\ w_v \\ w_h \end{pmatrix} \quad \text{and} \quad u = \begin{pmatrix} u_v \\ u_h \end{pmatrix}$$

for the state space representation. The state space representation can be written as

$$\dot{x} = A(x)x + B(x)u \tag{2.35a}$$

$$y = Cx + Du \tag{2.35b}$$

where

$$A(x) = \left(\begin{array}{ccccc} 0 & 1 & 0 & 0 & 0 \\ \frac{g[(A-B)\cos(a_v) - C\sin(a_v)]}{J_v a_v} & -\frac{k_{fv}}{J_v} & 0 & -\frac{H\sin(a_v)\cos(a_v)\dot{a}_h}{J_v} & \frac{l_m F_v(w_v)}{J_v} \\ 0 & 0 & 0 & 1 & 0 \\ 0 & 0 & 0 & -\frac{k_{fh}}{J_h} & -[\frac{k_m \sin(a_v)\dot{a}_v}{J_h} + \frac{k_m \cos(a_v)}{T_v J_h}] \\ 0 & 0 & 0 & 0 & -\frac{1}{T_v} \\ 0 & 0 & 0 & 0 & 0 \end{array} \right.$$

$$\left.\begin{matrix} 0 \\ -\frac{k_t}{J_v T_h} \\ 0 \\ \frac{l_t F_h(w_h)}{J_h} \\ 0 \\ -\frac{1}{T_h} \end{matrix}\right) \tag{2.36a}$$

$$B(x) = \begin{pmatrix} 0 & 0 \\ 0 & \frac{k_t}{J_v K_h} \\ 0 & 0 \\ \frac{k_m \cos(a_v)}{J_h K_v} & 0 \\ \frac{1}{K_v} & 0 \\ 0 & \frac{1}{K_h} \end{pmatrix} \tag{2.36b}$$

$$C = \begin{pmatrix} 1 & 0 & 0 & 0 & 0 & 0 \\ 0 & 0 & 1 & 0 & 0 & 0 \end{pmatrix} \tag{2.36c}$$

$$D = 0 \tag{2.36d}$$

It can be deduced from equation (2.3) that the propulsive forces of the propellers depend on angular velocity nonlinearly. In quasi-LPV modeling, this relationship between propulsive force and the angular velocity is assumed to be linear and therefore, we take

$$F_{v/h} = \widetilde{k}_{pv/h} w_{v/h}. \tag{2.37}$$

This assumption is useful to reduce the number of parameters in quasi-LPV model.

If we define a parameter vector as

$$p = \begin{pmatrix} p_1 \\ p_2 \\ p_3 \\ p_4 \\ p_5 \end{pmatrix} := \begin{pmatrix} a_v \\ \cos(a_v) \\ \sin(a_v) \\ \dot{a}_h \\ \dot{a}_v \end{pmatrix}, \tag{2.38}$$

we can then write

$$A(p) = \begin{pmatrix} 0 & 1 & 0 & 0 & 0 & 0 \\ \frac{g[(A-B)p_2 - Cp_3]}{J_v p_1} & -\frac{k_{fv}}{J_v} & 0 & -\frac{H p_3 p_2 p_4}{J_v} & \frac{l_m \widetilde{k}_{pv}}{J_v} & -\frac{k_t}{J_v T_h} \\ 0 & 0 & 0 & 1 & 0 & 0 \\ 0 & 0 & 0 & -\frac{k_{fh}}{J_h} & -[\frac{k_m p_3 p_5}{J_h} + \frac{k_m p_2}{T_v J_h}] & \frac{l_t \widetilde{k}_{ph}}{J_h} \\ 0 & 0 & 0 & 0 & -\frac{1}{T_v} & 0 \\ 0 & 0 & 0 & 0 & 0 & -\frac{1}{T_h} \end{pmatrix} \tag{2.39a}$$

$$B(p) = \begin{pmatrix} 0 & 0 \\ 0 & \frac{k_t}{J_v K_h} \\ 0 & 0 \\ \frac{k_m p_2}{J_h K_v} & 0 \\ \frac{1}{K_v} & 0 \\ 0 & \frac{1}{K_h} \end{pmatrix} \tag{2.39b}$$

$$C = \begin{pmatrix} 1 & 0 & 0 & 0 & 0 & 0 \\ 0 & 0 & 1 & 0 & 0 & 0 \end{pmatrix} \tag{2.39c}$$

$$D = 0 \tag{2.39d}$$

The nonlinear system represented in equation (2.35a) thus becomes a parameter dependent system as

$$
\begin{aligned}
\dot{x} &= A(p)x + B(p)u && \text{(2.40a)}\\
y &= Cx + Du. && \text{(2.40b)}
\end{aligned}
$$

In mathematics, a polynomial is an expression constructed from one or more variables and constants, using the operations of addition, subtraction, multiplication, and raising to constant non-negative integer powers. Moreover, a rational function is any function which can be written as the ratio of two polynomial functions. It can be observed from equation (2.39) that the parameter dependence of the TRMS is in the form of ratios of polynomials. Such systems are referred to as *Linear Fractional LPV (LF-LPV) systems.* In the next chapter, we discuss LF-LPV systems in detail.

3. Linear Fractional Representations

Most engineering problems, especially control problems, begin with the modeling of the system. It is also same for some division of the sociology and economy. However, the success of the study mostly depends on the closeness of the model and the real system. The model of the system should contain all possibilities of the real system. For instance; car suspension design. What is the mass of the car? Should the mass of the car be taken with passengers or without passengers? How can this uncertainty be taken into consideration in the design? Indeed, Linear Parameter Varying system can be considered as this example. This method enable to take into consideration all uncertainties in the system.

In general LPV systems are represented as,

$$\dot{x} = A(p)x + B(p)u \tag{3.1a}$$

$$y = C(p)x + D(p)u \tag{3.1b}$$

where $p = (p_1, \cdots, p_k)^T$ is the vector of time-varying parameters, where each p_i is bounded as $p_i(t) \in [\underline{p}_i, \overline{p}_i]$ for all t.

A ratio of polynomials in one or more variables is referred to as a *rational*, or *linear fractional* function. Hence, if the parameter dependence is in the form of a ratio of polynomials, we say the system is a linear fractional LPV system. As pointed out at the end of the previous chapter, the TRMS system is linear-fractional LPV in terms of the parameters $p_1, \cdots, p_5$. We now look at rational functions and the so-called Linear Fractional Transformation (LFT) in some detail.

3.1. Linear Fractional Transformation (LFT)

We begin by a simple example.

Example 3.1.1. *[8] Consider the static system*

$$y = \frac{d + \delta(bc - ad)}{1 - a\delta} u =: K(\delta)u. \tag{3.2}$$

We can express $K(\delta)$ as

$$\begin{aligned} K(\delta) &= \frac{d(1 - a\delta) + bc\delta}{1 - a\delta} \\ &= d + c\delta(1 - a\delta)^{-1}b. \end{aligned} \tag{3.3}$$

A straightforward calculation shows that we can represent the system as

$$\begin{pmatrix} z_u \\ y \end{pmatrix} = \begin{pmatrix} a & b \\ c & d \end{pmatrix} \begin{pmatrix} w_u \\ u \end{pmatrix} \tag{3.4}$$

$$\text{where} \quad w_u = \delta z_u. \tag{3.5}$$

We can express (3.4) and (3.5) equivalently as a feedback interconnection shown in Figure 3.1.

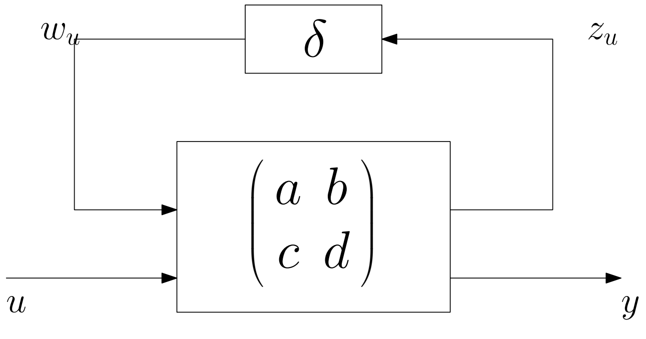

Figure 3.1. Representation of $K(\delta)$

The Example 3.1.1 is a simple situation for a parameter dependent system. In general, parameter dependent systems can be shown as in Figure 3.2. The LFT representation of any rational parameter dependent system is the interconnection of the parameter variation

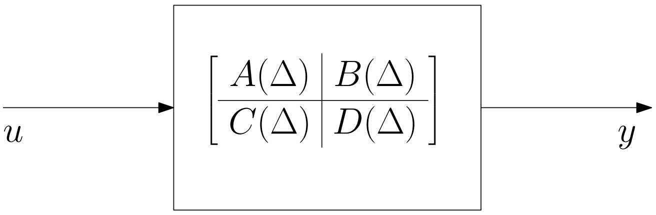
$\left[\begin{array}{c|c} A(\Delta) & B(\Delta) \\ \hline C(\Delta) & D(\Delta) \end{array}\right]$
u
y

Figure 3.2. Parameter Dependent State-Space Representation

and the nominal Linear Time Invariant (LTI) system. The variation of the parameters are pulled out from the nominal system and they are collected in the Δ block. This LFT interconnection is represented in Figure 3.3. The equations of the LFT interconnection represented in Figure 3.3 are written as

$$\begin{aligned} \dot{x} &= Ax + B_1 w + B_2 u && (3.6a) \\ z &= C_1 x + D_{11} w + D_{12} u \quad \text{uncertainty channel} && (3.6b) \\ y &= C_2 x + D_{21} w + D_{22} u \quad \text{input - output channel} && (3.6c) \end{aligned}$$

where

$$w = \Delta z. \tag{3.7}$$

The structure of the Δ block is described as

$$\boldsymbol{\Delta} = \mathrm{diag}(\delta_1 I_{n_1}, \cdots, \delta_k I_{n_k}). \tag{3.8}$$

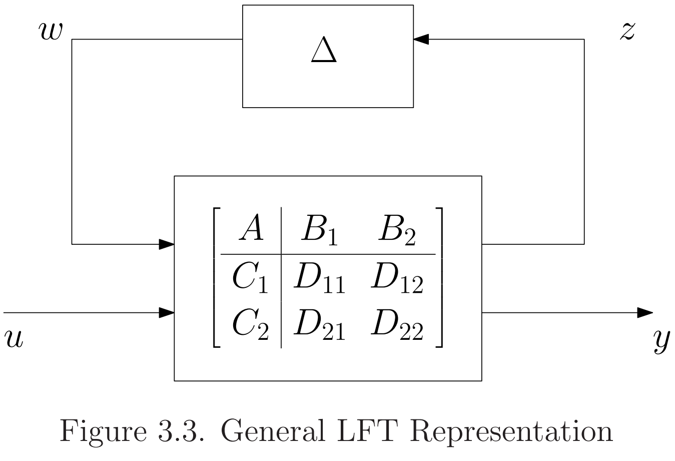
w
Δ
z
$\left[\begin{array}{c|cc} A & B_1 & B_2 \\ \hline C_1 & D_{11} & D_{12} \\ C_2 & D_{21} & D_{22} \end{array}\right]$
u
y

Figure 3.3. General LFT Representation

$\delta_1, \cdots, \delta_k$ are the variations of the parameters. $n_1, \cdots, n_k$ indicate how many times a parameter is seen in the system. As mentioned in the beginning of the chapter, the variations of the parameters are bounded with finite values. However, this variations can be normalized for desired bounds. We will discuss normalization method in detail in *Normalization of the Parameters* section. For that purpose, a specific Δ block set is defined as

Definition 3.1.1. *The* unit ball *set is defined as*

$$\boldsymbol{B}_\Delta := \{\Delta \in \boldsymbol{\Delta} : \Delta^T \Delta \preceq I\}.$$

After the discussion of the structure of Δ, we can continue giving more information about LFTs. There are two different types of LFT interconnections:

- Upper-LFT as illustrated in Figure 3.4
- Lower-LFT as illustrated in Figure 3.5

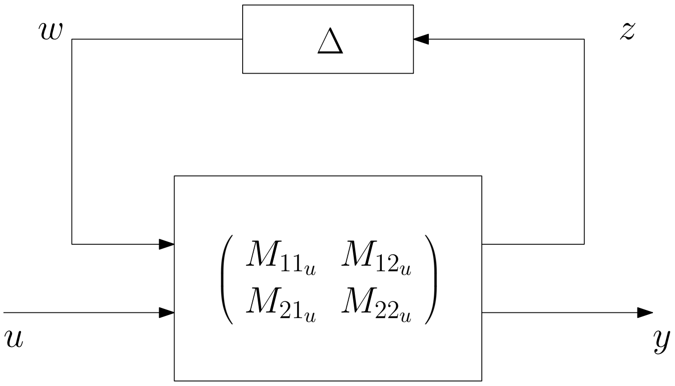
w
Δ
z
$\begin{pmatrix} M_{11_u} & M_{12_u} \\ M_{21_u} & M_{22_u} \end{pmatrix}$
u
y

Figure 3.4. Simplified LFT Representation (Upper)

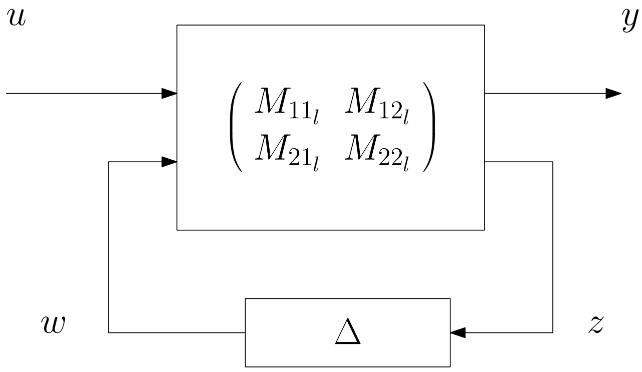
u
y
$\begin{pmatrix} M_{11_l} & M_{12_l} \\ M_{21_l} & M_{22_l} \end{pmatrix}$
w
Δ
z

Figure 3.5. Simplified LFT Representation (Lower)

The transfer between u and y is denoted as $F_u(M,\Delta)$ for upper-LFT and $F_l(M,\Delta)$ for lower-LFT. Specifically,

$$\begin{aligned} F_u(M_u,\Delta) &= M_{21_u}\Delta(I - M_{11_u}\Delta)^{-1}M_{12_u} + M_{22_u} && \text{(3.9a)} \\ F_l(M_l,\Delta) &= M_{12_l}\Delta(I - M_{22_l}\Delta)^{-1}M_{21_l} + M_{11_l}, && \text{(3.9b)} \end{aligned}$$

where

$$\begin{aligned} M_u &:= \begin{pmatrix} M_{11_u} & M_{12_u} \\ M_{21_u} & M_{22_u} \end{pmatrix} && \text{(3.10a)} \\ M_l &:= \begin{pmatrix} M_{11_l} & M_{12_l} \\ M_{21_l} & M_{22_l} \end{pmatrix} && \text{(3.10b)} \end{aligned}$$

For upper-LFT representation, unless $M_{11_u} = 0$ the matrix $(I - M_{11_u}\Delta)$ cannot be inverted for all values $\Delta \in \mathbf{\Delta}$. In fact, it is sufficient that invertibility is feasible for all $\Delta \in \mathbf{B}_\Delta$. We call the LFT well-posed, if

$$det(I - M_{11_u}\Delta) \neq 0 \quad \text{for all} \quad \Delta \in \mathbf{B}_\Delta. \tag{3.11}$$

We assume that systems, indicated in this thesis, are well-posed.

At the end of this section, the following example is useful to show the derivation of LFT representation. This example is more complex than Example 3.1.1. In this example, we consider a *mass-spring-damper* system. The damper constant c and the spring constant k are the time varying parameters of the system. Firstly, we derive the mathematical model of the system. The model depends on the parameters c and k. The variations of the parameters are pull out from the system by putting the nominal values of the parameters and their variations in the system. Finally, Δ block is constructed and it is interconnected with the nominal system.

Example 3.1.2. *[10] In this example, the spring constant k and the damping ratio c are* *the parameters which are changing between*

$$\begin{aligned} k &= [\underline{k}, \overline{k}] && (3.12a) \\ c &= [\underline{c}, \overline{c}] && (3.12b) \end{aligned}$$

The equation of motion of the system

$$m\ddot{\xi} + c\dot{\xi} + k\xi = F \tag{3.13}$$

The nominal values of the parameters can be defined as the geometric mean of the bounds.

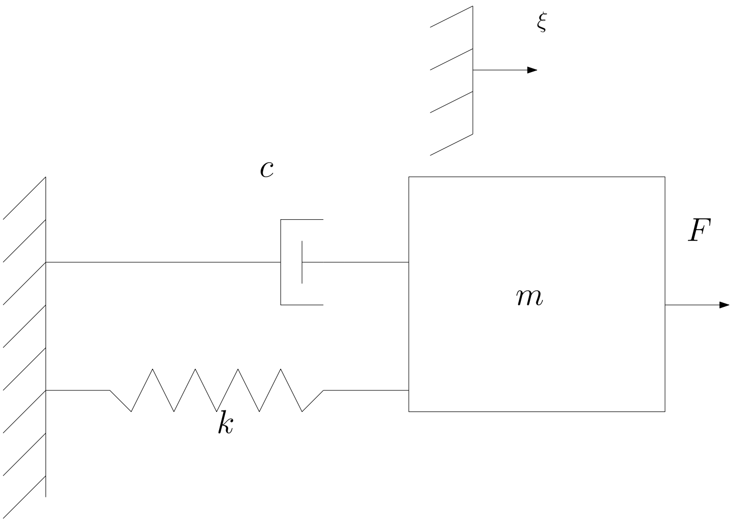

Figure 3.6. Mass-Spring-Damper System

$$\begin{aligned} k_o &:= \tfrac{\overline{k}+\underline{k}}{2} && (3.14a) \\ c_o &:= \tfrac{\overline{c}+\underline{c}}{2} && (3.14b) \end{aligned}$$

Then, we can write the variations of the parameters as,

$$\begin{aligned} k_v &:= \overline{k} - k_o && (3.15a) \\ c_v &:= \overline{c} - c_o && (3.15b) \end{aligned}$$

When we put the nominal values and the variations of the parameters into the system.

Equation of motion can be rewritten as

$$\underbrace{m\ddot{\xi}+c_o\dot{\xi}+k_o\xi}_{nominalsystem} = F+c_v\dot{\xi}+k_v\xi, \quad z_c := \dot{\xi} \quad and \quad z_k := \xi \tag{3.16a}$$

$$= F+z_cc_v+z_kk_v, \quad z_cc_v = w_c \quad and \quad z_kk_v = w_k \tag{3.16b}$$

$$= F+w_c+w_k \tag{3.16c}$$

Then we can write

$$\begin{pmatrix} \dot{\xi} \\ \ddot{\xi} \end{pmatrix} = \begin{pmatrix} 0 & 1 \\ -\frac{k_o}{m} & -\frac{c_o}{m} \end{pmatrix} \begin{pmatrix} \xi \\ \dot{\xi} \end{pmatrix} + \begin{pmatrix} 0 & 0 \\ \frac{1}{m} & \frac{1}{m} \end{pmatrix} \begin{pmatrix} w_k \\ w_c \end{pmatrix} + \begin{pmatrix} 0 \\ \frac{1}{m} \end{pmatrix} F \tag{3.17a}$$

$$\begin{pmatrix} z_k \\ z_c \end{pmatrix} = \begin{pmatrix} 1 & 0 \\ 0 & 1 \end{pmatrix} \begin{pmatrix} \xi \\ \dot{\xi} \end{pmatrix} \tag{3.17b}$$

$$\begin{pmatrix} w_k \\ w_c \end{pmatrix} = \begin{pmatrix} k_v & 0 \\ 0 & c_v \end{pmatrix} \begin{pmatrix} z_k \\ z_c \end{pmatrix} \tag{3.17c}$$

In block diagram form

$$\begin{pmatrix} \dot{\xi} \\ \ddot{\xi} \\ z_k \\ z_c \\ y \end{pmatrix} = \underbrace{\left(\begin{array}{cc:cc:c} 0 & 1 & 0 & 0 & 0 \\ -\frac{k_o}{m} & -\frac{c_o}{m} & \frac{1}{m} & \frac{1}{m} & \frac{1}{m} \\ \hdashline 1 & 0 & 0 & 0 & 0 \\ 0 & 1 & 0 & 0 & 0 \\ \hdashline 1 & 0 & 0 & 0 & 0 \end{array}\right)}_{M} \begin{pmatrix} \xi \\ \dot{\xi} \\ w_k \\ w_c \\ F \end{pmatrix} \tag{3.18a}$$

$$\begin{pmatrix} w_k \\ w_c \end{pmatrix} = \underbrace{\begin{pmatrix} k_v & 0 \\ 0 & c_v \end{pmatrix}}_{\Delta} \begin{pmatrix} z_k \\ z_c \end{pmatrix} \tag{3.18b}$$

$$F_u(M,\Delta) = \underbrace{\begin{pmatrix} 1 & 0 \\ 0 & 1 \\ \hdashline 1 & 0 \end{pmatrix}}_{M_{21}} \cdot \underbrace{\begin{pmatrix} k_v & 0 \\ 0 & c_v \end{pmatrix}}_{\Delta} \left(I - \underbrace{\begin{pmatrix} 0 & 1 \\ \frac{k_o}{m} & \frac{c_o}{m} \end{pmatrix}}_{M_{11}} \underbrace{\begin{pmatrix} k_v & 0 \\ 0 & c_v \end{pmatrix}}_{\Delta} \right)^{-1} \underbrace{\left(\begin{array}{cc:c} 0 & 0 & 0 \\ \frac{1}{m} & \frac{1}{m} & \frac{1}{m} \end{array}\right)}_{M_{12}} + \underbrace{\left(\begin{array}{cc:c} 0 & 0 & 0 \\ 0 & 0 & 0 \\ \hdashline 0 & 0 & 0 \end{array}\right)}_{M_{22}} \qquad (3.19)$$

3.2. Normalization of the Parameters

For analysis which is used for uncertain systems, it is generally better to normalize the parameter variations between -1 and +1. For instance, the system depends on two parameters δ_1 and δ_2 with $\delta_1 \in [\delta_1^-, \delta_1^+]$ and $\delta_2 \in [\delta_2^-, \delta_2^+]$ normalizing consists of replacing δ_1, δ_2 by $\acute{\delta}_1, \acute{\delta}_2$

$$\delta_1 = \frac{\delta_1^+ + \delta_1^-}{2} + \frac{\delta_1^+ - \delta_1^-}{2}\acute{\delta}_1 \qquad (3.20a)$$

$$\delta_2 = \frac{\delta_2^+ + \delta_2^-}{2} + \frac{\delta_2^+ - \delta_2^-}{2}\acute{\delta}_2 \qquad (3.20b)$$

where $\acute{\delta}_1 \in [-1, +1]$ and $\acute{\delta}_2 \in [-1, +1]$.

More generally, n_1 and n_2 are the number of parameters seen in the system model and normalization consists of replacing Δ by $P\acute{\Delta}Q + R$. The expression of P, Q and R in the above example is

$$P = \begin{pmatrix} I_{n1} & 0 \\ 0 & I_{n2} \end{pmatrix} ; Q = \begin{pmatrix} I_{n1}\frac{\delta_1^+ - \delta_1^-}{2} & 0 \\ 0 & I_{n2}\frac{\delta_2^+ - \delta_2^-}{2} \end{pmatrix} ; R = \begin{pmatrix} I_{n1}\frac{\delta_1^+ + \delta_1^-}{2} & 0 \\ 0 & I_{n2}\frac{\delta_2^+ + \delta_2^-}{2} \end{pmatrix}$$

The following lemma computes the new equivalent expression to normalize the system

Lemma 3.2.1. *If the matrix Δ is replaced by $P\acute{\Delta}Q+R$, the following expression is obtained*

$$F_u(M, \Delta) = F_u(\acute{M}, \acute{\Delta}) \tag{3.21}$$

provided that

$$\begin{aligned}
\acute{M}_{11} &= Q(I - M_{11}R)^{-1}M_{11}P && \text{(3.22a)}\\
\acute{M}_{12} &= Q(I - M_{11}R)^{-1}M_{12} && \text{(3.22b)}\\
\acute{M}_{21} &= M_{21}P + M_{21}R(I - M_{11R})^{-1}M_{11}P && \text{(3.22c)}\\
\acute{M}_{22} &= M_{22}P + M_{21}R(I - M_{11R})^{-1}M_{12} && \text{(3.22d)}
\end{aligned}$$

The presented normalization procedure can be applied to Example 3.1.2

Example 3.2.1. *The parameters k and c can be normalized as follows*

$$k = k_o - \acute{k}\delta_k, \quad \delta_k = [-1, +1] \textit{ where } k_o := \frac{\overline{k} + \underline{k}}{2} \textit{ and } \acute{k} := -\frac{\overline{k} - \underline{k}}{2} \tag{3.23a}$$

and

$$c = c_o - \acute{c}\delta_k, \quad \delta_c = [-1, +1] \textit{ where } c_o := \frac{\overline{c} + \underline{c}}{2} \textit{ and } \acute{c} := -\frac{\overline{c} - \underline{c}}{2} \tag{3.23b}$$

Then we can rewrite the equation of motion as

$$\begin{aligned}
\underbrace{m\ddot{\xi} + c_o\dot{\xi} + k_o\xi}_{nominal system} &= F + \acute{c}\delta_c\dot{\xi} + \acute{k}\delta_k\xi, \quad z_c = \acute{c}\xi \quad \textit{and} \quad z_k = \acute{k}\xi && \text{(3.24a)}\\
&= F + z_c\delta_c + z_k\delta_k, \quad z_c\delta_c = w_c \quad \textit{and} \quad z_k\delta_k = w_k && \text{(3.24b)}\\
&= F + w_c + w_k && \text{(3.24c)}
\end{aligned}$$

Then we can write

$$\begin{pmatrix} \dot{\xi} \\ \ddot{\xi} \end{pmatrix} = \begin{pmatrix} 0 & 1 \\ -\frac{k_o}{m} & -\frac{c_o}{m} \end{pmatrix} \begin{pmatrix} \xi \\ \dot{\xi} \end{pmatrix} + \begin{pmatrix} 0 & 0 \\ \frac{1}{m} & \frac{1}{m} \end{pmatrix} \begin{pmatrix} w_k \\ w_c \end{pmatrix} + \begin{pmatrix} 0 \\ \frac{1}{m} \end{pmatrix} F \tag{3.25a}$$

$$\begin{pmatrix} z_k \\ z_c \end{pmatrix} = \begin{pmatrix} \acute{k} & 0 \\ 0 & \acute{c} \end{pmatrix} \begin{pmatrix} \xi \\ \dot{\xi} \end{pmatrix} \tag{3.25b}$$

$$\begin{pmatrix} w_k \\ w_c \end{pmatrix} = \begin{pmatrix} \delta_k & 0 \\ 0 & \delta_c \end{pmatrix} \begin{pmatrix} z_k \\ z_c \end{pmatrix} \tag{3.25c}$$

In block diagram form

$$\begin{pmatrix} \dot{\xi} \\ \ddot{\xi} \\ z_k \\ z_c \\ y \end{pmatrix} = \underbrace{\left(\begin{array}{cc|cc|c} 0 & 1 & 0 & 0 & 0 \\ -\frac{k_o}{m} & -\frac{c_o}{m} & \frac{1}{m} & \frac{1}{m} & \frac{1}{m} \\ \hline \acute{k} & 0 & 0 & 0 & 0 \\ 0 & \acute{c} & 0 & 0 & 0 \\ \hline 1 & 0 & 0 & 0 & 0 \end{array}\right)}_{M} \begin{pmatrix} \xi \\ \dot{\xi} \\ w_k \\ w_c \\ F \end{pmatrix} \tag{3.26a}$$

$$\begin{pmatrix} w_k \\ w_c \end{pmatrix} = \underbrace{\begin{pmatrix} \delta_k & 0 \\ 0 & \delta_c \end{pmatrix}}_{\Delta} \begin{pmatrix} z_k \\ z_c \end{pmatrix} \tag{3.26b}$$

$$F_u(M,\Delta) = \underbrace{\left(\begin{array}{cc} \acute{k} & 0 \\ 0 & \acute{c} \\ \hline 1 & 0 \end{array}\right)}_{M_{21}} \underbrace{\begin{pmatrix} \delta_k & 0 \\ 0 & \delta_c \end{pmatrix}}_{\Delta} \left(I - \underbrace{\begin{pmatrix} 0 & 1 \\ \frac{k_o}{m} & \frac{c_o}{m} \end{pmatrix}}_{M_{11}} \underbrace{\begin{pmatrix} \delta_k & 0 \\ 0 & \delta_c \end{pmatrix}}_{\Delta} \right)^{-1} \underbrace{\left(\begin{array}{cc|c} 0 & 0 & 0 \\ \frac{1}{m} & \frac{1}{m} & \frac{1}{m} \end{array}\right)}_{M_{12}} + \underbrace{\left(\begin{array}{cc|c} 0 & 0 & 0 \\ 0 & 0 & 0 \\ \hline 0 & 0 & 0 \end{array}\right)}_{M_{22}} \tag{3.27}$$

As mentioned in the beginning of the chapter, if the time varying parameters are in the rational polynomial form in the equation, this system can be represented in LFT form. The LFT representation of the parameter dependent systems are used to design a controller for the system. As mentioned before, LFR Toolbox presents useful functions to obtain the LFT representation of a parameter dependent system. We will discuss functions of the LFR Toolbox and the LFT representation of the TRMS in detail. In the next chapter, stability and the performance analysis of the LF-LPV systems are discussed and the procedure of the controller design is presented.

4. LF-LPV Systems: Analysis and Control Design

In first the section of the chapter, we will discuss the stability and the performance analysis of the LF-LPV systems. The stability conditions of a parameter dependent system will be presented in terms of LMIs. In the second section, control design will be discussed and we will show the solution of the controller.

4.1. Analysis of LF-LPV Systems

The main idea of the stability condition in terms of LMIs comes from the Lyapunov equation. This idea can be considered for an autonomous system in the following theorem

Theorem 4.1.1. *[6] The system $\dot{x} = Ax$ is asymptotically stable if and only if there exists a solution $P = P^T \succ 0$ to the inequality*

$$A^T P + PA \prec 0.$$

Consider the system

$$\dot{x} = Ax + B_1 \tag{4.1a}$$

$$w_u = C_1 x + D_{11} z_u, \qquad w_u = \Delta z_u. \tag{4.1b}$$

The illustration of the system is presented in Figure 4.1.

We assume A is Hurwitz and Δ is in the form (3.8). The following theorem gives sufficient conditions that guarantee robust stability for all admissible parameter trajectories.

Theorem 4.1.2. *[7] The system 4.1 is robustly stable if there exists an $X = X^T \succ 0$ and*

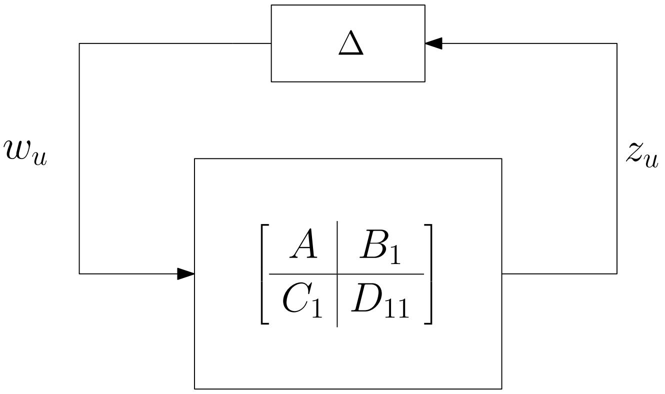
Δ
w_u
z_u
$\left[\begin{array}{c|c} A & B_1 \\ \hline C_1 & D_{11} \end{array}\right]$

Figure 4.1. LF-LPV System without Performance Channel

matrices $Q = Q^T$, S and $R = R^T$ such that

$$\begin{pmatrix} I & 0 \\ A & B_1 \\ \hline 0 & I \\ C_1 & D_{11} \end{pmatrix}^T \left(\begin{array}{cc|cc} 0 & X & 0 & 0 \\ X & 0 & 0 & 0 \\ \hline 0 & 0 & Q & S \\ 0 & 0 & S^T & R \end{array}\right) \begin{pmatrix} I & 0 \\ A & B_1 \\ \hline 0 & I \\ C_1 & D_{11} \end{pmatrix} \prec 0 \tag{4.2}$$

and

$$\begin{pmatrix} \Delta \\ I \end{pmatrix}^T \begin{pmatrix} Q & S \\ S^T & R \end{pmatrix} \begin{pmatrix} \Delta \\ I \end{pmatrix} \succ 0 \quad \textit{for all} \quad \Delta \in \mathbf{\Delta}. \tag{4.3}$$

System (4.1) is a parameter dependent autonomous system. However, this idea can be extended to quantify the effect of the disturbance on the system. This way, system can remain still stable for reasonable disturbance from the environment. The extra channel is added to the system (4.1) called the *Performance Channel.* This way, we can obtain the system (4.4).

$$\dot{x} = Ax + B_1 w_u + B_p w_p \tag{4.4a}$$

$$z_u = C_1 x + D_{11} w_u + D_{1p} w_p, \qquad w_u = \Delta z_u \tag{4.4b}$$

$$z_p = C_p x + D_{1p} w_u + D_{pp} w_p \tag{4.4c}$$

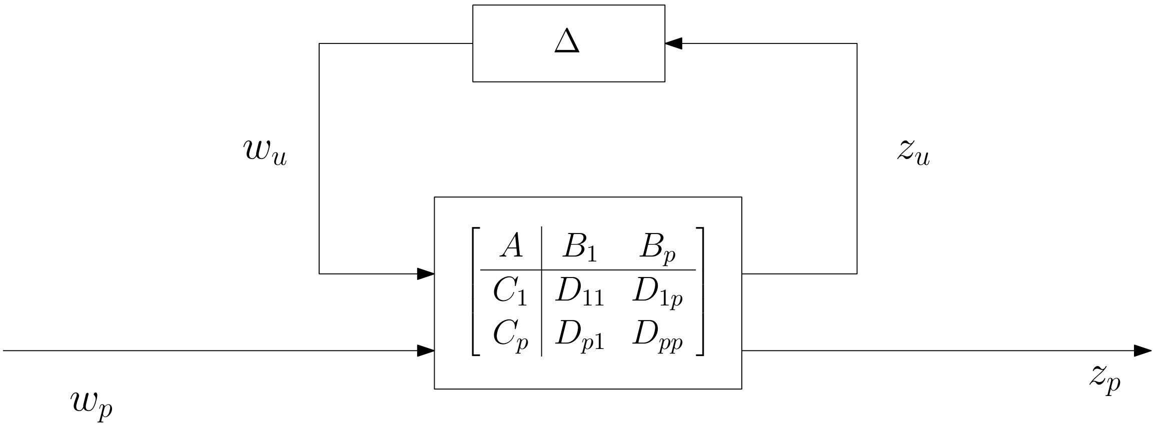

Δ
w_u
z_u
$\left[\begin{array}{c|cc} A & B_1 & B_p \\ \hline C_1 & D_{11} & D_{1p} \\ C_p & D_{p1} & D_{pp} \end{array}\right]$
w_p
z_p

Figure 4.2. LF-LPV System with Performance Channel

The system with performance channel is shown in Figure 4.2.

In system (4.4), w_p (disturbance) is seen as an input variable whose effect on the output z_p we try to minimize. The effect of the w_p on z_p can be quantified by calculating the worst possible ratio of their norms. A norm is a function that assigns a strictly positive length or size to all vectors in a vector space, other than the zero vector. In other words, we can measure the size of vectors by taking their norms. Here, we will use the L_2-norm (a.k.a. the *energy-norm*) for analysis.

Definition 4.1.1. *[10] The L_2 norm of the vector $x(t) = (x_1(t), \cdots, x_n(t))^T$ is defined as*

$$\|x\|_2 = \sqrt{\int_0^\infty x^T(t)x(t).dt} \tag{4.5}$$

Based on Figure 4.3, the L_2-gain system from w_p to z_p can be represented as

$$\|T\|_{L_2 \to L_2} := \sup_{w_p \in L_2, w_p \neq 0} \frac{\|z_p\|_2}{\|w_p\|_2} \tag{4.6}$$

The following theorem gives the conditions for which LPV system (4.4) remains stable with L_2 norm below γ.

Theorem 4.1.3. *[7] Consider the system 4.4. Assume that A is Hurwitz and $\gamma > 0$. Then, the LPV system 4.4 remains stable with L_2 norm below γ if there exists an $X = X^T \succ 0$*

and matrices $Q = Q^T$, S *and* $R = R^T$ *such that*

$$\left(\begin{array}{ccc} I & 0 & 0 \\ A & B_1 & B_p \\ \hline 0 & I & 0 \\ C_1 & D_{11} & D_{1p} \\ \hline 0 & 0 & I \\ C_p & D_{p1} & D_{p2} \end{array}\right)^T \left(\begin{array}{cc|cc|cc} 0 & X & 0 & 0 & 0 & 0 \\ X & 0 & 0 & 0 & 0 & 0 \\ \hline 0 & 0 & Q & S & 0 & 0 \\ 0 & 0 & S^T & R & 0 & 0 \\ \hline 0 & 0 & 0 & 0 & -\gamma I & 0 \\ 0 & 0 & 0 & 0 & 0 & \gamma^{-1} I \end{array}\right) \left(\begin{array}{ccc} I & 0 & 0 \\ A & B_1 & B_p \\ \hline 0 & I & 0 \\ C_1 & D_{11} & D_{1p} \\ \hline 0 & 0 & I \\ C_p & D_{p1} & D_{p2} \end{array}\right) \prec 0 \qquad (4.7)$$

and

$$\begin{pmatrix} \Delta \\ I \end{pmatrix}^T \begin{pmatrix} Q & S \\ S^T & R \end{pmatrix} \begin{pmatrix} \Delta \\ I \end{pmatrix} \succ 0 \quad \textit{for all} \quad \Delta \in \mathbf{\Delta}. \qquad (4.8)$$

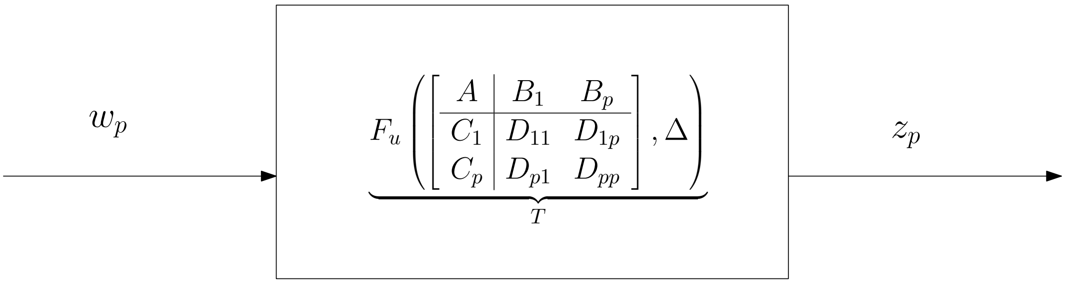
w_p
$\underbrace{F_u\left(\left[\begin{array}{c|cc} A & B_1 & B_p \\ \hline C_1 & D_{11} & D_{1p} \\ C_p & D_{p1} & D_{pp} \end{array}\right], \Delta\right)}_{T}$
z_p

Figure 4.3. Transfer between w_p and z_p

4.2. Control Design for LF-LPV Systems

In this section, we will discuss the controller design for LF-LPV system. In the previous section, the stability and performance conditions are given in Theorems 4.1.3 and 4.1.2.

Now consider the systems with a control input u, and a measured output y which is illustrated in Figure 4.4. The system equations are

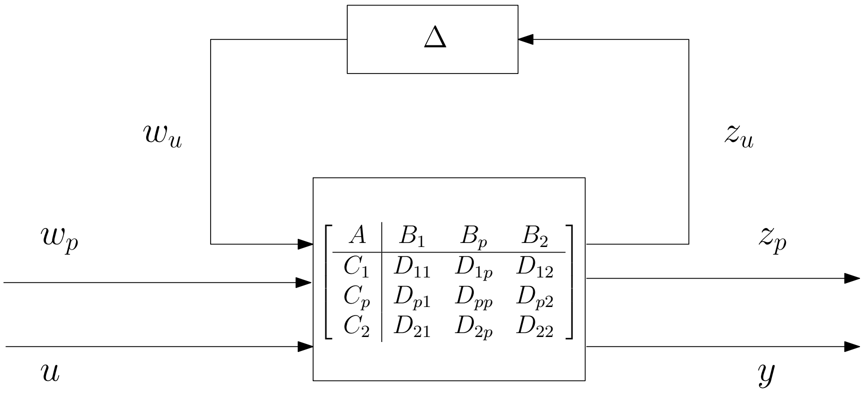
Δ
w_u
z_u
w_p
z_p
u
y
$\left[\begin{array}{c|ccc} A & B_1 & B_p & B_2 \\ \hline C_1 & D_{11} & D_{1p} & D_{12} \\ C_p & D_{p1} & D_{pp} & D_{p2} \\ C_2 & D_{21} & D_{2p} & D_{22} \end{array}\right]$

Figure 4.4. LF-LPV system with control input u and measured output y

$$\dot{x} = Ax + B_1 w_u + B_p w_p + B_2 u \tag{4.9a}$$

$$z_u = C_1 x + D_{11} w_u + D_{1p} w_p + D_{12} u, \qquad w_u = \Delta z_u \tag{4.9b}$$

$$z_p = C_p x + D_{p1} z_u + D_{pp} z_p + D_{p2} u \tag{4.9c}$$

$$y = C_2 x + D_{21} w_u + D_{2p} w_p. \tag{4.9d}$$

The objective is to design a controller of the form

$$\dot{x}_K = A_K x_K + B_{K_2} y + B_{K_1} w_{K_u} \tag{4.10a}$$

$$u = C_{K_2} x_K + D_{K_{22}} y + D_{K_{21}} w_{K_u} \tag{4.10b}$$

$$z_{K_u} = C_{K_1} x_K + D_{K_{12}} y + D_{K_{11}} w_{K_u}, \qquad w_{K_u} = \Delta z_{K_u}. \tag{4.10c}$$

Figure 4.5 shows the form of the desired controller.

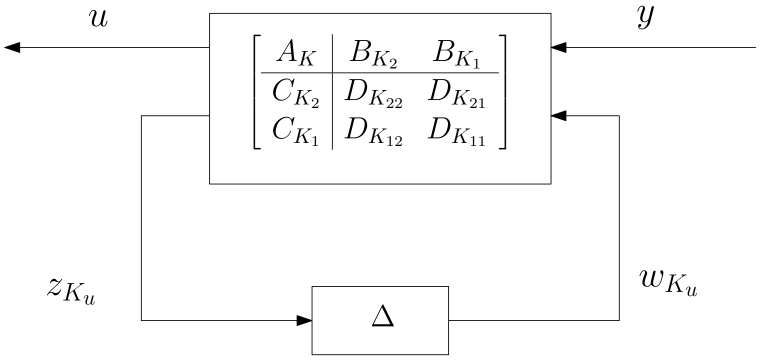
u
y
$\left[\begin{array}{c|cc} A_K & B_{K_2} & B_{K_1} \\ \hline C_{K_2} & D_{K_{22}} & D_{K_{21}} \\ C_{K_1} & D_{K_{12}} & D_{K_{11}} \end{array}\right]$
z_{K_u}
w_{K_u}
Δ

Figure 4.5. The Illustration of Controller

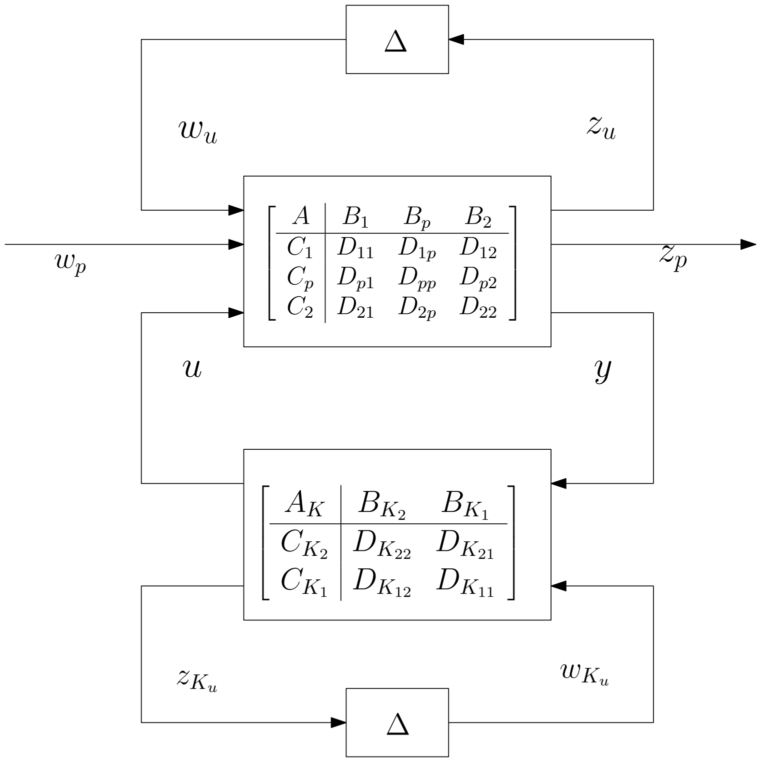
Δ
w_u
z_u
$\left[\begin{array}{c|ccc} A & B_1 & B_p & B_2 \\ \hline C_1 & D_{11} & D_{1p} & D_{12} \\ C_p & D_{p1} & D_{pp} & D_{p2} \\ C_2 & D_{21} & D_{2p} & D_{22} \end{array}\right]$
w_p
z_p
u
y
$\left[\begin{array}{c|cc} A_K & B_{K_2} & B_{K_1} \\ \hline C_{K_2} & D_{K_{22}} & D_{K_{21}} \\ C_{K_1} & D_{K_{12}} & D_{K_{11}} \end{array}\right]$
z_{K_u}
w_{K_u}
Δ

Figure 4.6. The Closed Loop System

When the plant and the controller are combined, we obtain the closed loop system as [9]

$$\dot{x}^a = (A^a + B_2^a K C_2^a)x^a + (B_1^a + B_2^a K D_{21}^a)w_u^a + B_p^a w_p \tag{4.11a}$$

$$z_u^a = (C_1^a + D_{12}^a K C_2^a)x^a + (D_{11}^a + D_{12}^a K D_{21}^a)w_u^a + D_{1p}^a w_p \tag{4.11b}$$

$$z_p = (C_p^a + D_{p2}^a K C_2^a)x^a + (D_{p1}^a + D_{p2}^a K D_{21}^a)w_u^a + D_{pp}^a w_p \tag{4.11c}$$

Where

$$A^a := \begin{pmatrix} A & 0 \\ 0 & 0 \end{pmatrix},\ B_2^a := \begin{pmatrix} B_2 & 0 & 0 \\ 0 & 0 & I_n \end{pmatrix},\ B_1^a := \begin{pmatrix} C_2 & 0 \\ 0 & 0 \\ 0 & I_n \end{pmatrix},\ D_{p2}^a := \begin{pmatrix} D_{p2} & 0 & 0 \end{pmatrix}$$

$$C_p^a := \begin{pmatrix} C_p & 0 \end{pmatrix},\ D_{1p}^a := \begin{pmatrix} D_{1p} \\ 0 \end{pmatrix},\ D_{p1}^a := \begin{pmatrix} D_{p1} & 0 \end{pmatrix},\ D_{pp}^a = D_{pp},$$

$$B_1^a := \begin{pmatrix} B_1 & 0 \\ 0 & 0_{n\times m} \end{pmatrix},\ C_1^a := \begin{pmatrix} C_1 & 0 \\ 0 & 0_{m\times n} \end{pmatrix},\ D_{21}^a := \begin{pmatrix} D_{21} & 0 & D_{2p} \\ 0 & I_m & 0 \\ 0 & 0 & 0 \end{pmatrix} \tag{4.12}$$

$$D_{12}^a := \begin{pmatrix} D_{12} & 0 & 0 \\ 0 & I_m & 0 \end{pmatrix},\ D_{11}^a := \begin{pmatrix} D_{11} & 0 \\ 0 & 0_{m\times m} \end{pmatrix},\ K := \begin{pmatrix} D_{K_{22}} & D_{K_{21}} & C_{K_2} \\ D_{K_{12}} & D_{K_{11}} & C_{K_1} \\ B_{K_2} & B_{K_1} & A_K \end{pmatrix}$$

n is number of state and m is number of repeated parameters.

The closed loop matrices can be written in more compact form as

$$G_{cl} = \left[\begin{array}{c|c} A_{cl} & B_{cl} \\ \hline C_{cl} & D_{cl} \end{array}\right] \tag{4.13}$$

$$A_{cl} = A^a + B_2^a K C_2^a,\ B_{cl} = \widetilde{B}_1^a + B_2^a K D_{21} \tag{4.14}$$

$$C_{cl} = \widehat{C}_1^a + D_{12}^a K C_2^a,\ D_{cl} = \widetilde{D}_{11}^a + \widetilde{D}_{12}^a K D_{21}^a \tag{4.15}$$

where

$$\widetilde{B}_1^a := \begin{pmatrix} B_1^a & B_p^a \end{pmatrix},\ \widetilde{C}_1^a := \begin{pmatrix} C_1^a \\ C_p^a \end{pmatrix},\ \widetilde{D}_{11}^a := \begin{pmatrix} D_{11}^a & D_{1p}^a \\ D_{p1}^a & D_{pp}^a \end{pmatrix},\ \widetilde{D}_{12}^a := \begin{pmatrix} D_{12}^a \\ D_{p2}^a \end{pmatrix} \tag{4.16}$$

We can write the stability condition of the closed loop system by using Theorem 4.1.3. The closed loop system 4.11 remains stable with L_2 norm below $\gamma > 0$, if there exist $\chi = \chi^T \succ 0$,

$Q_e = Q_e^T \prec 0$, $R_e = R_e^T \succ 0$, and $\gamma > 0$ such that the inequalities [7]

$$\chi \succ 0, \begin{pmatrix} A_{cl} & B_{cl} \\ C_{cl} & D_{cl} \\ I & 0 \\ 0 & I \end{pmatrix}^T \begin{pmatrix} 0 & 0 & 0 & \chi & 0 & 0 \\ 0 & R_e & 0 & 0 & 0 & 0 \\ 0 & 0 & \gamma^{-1}I & 0 & 0 & 0 \\ \chi & 0 & 0 & 0 & 0 & 0 \\ 0 & 0 & 0 & 0 & Q_e & 0 \\ 0 & 0 & 0 & 0 & 0 & -\gamma I \end{pmatrix} \begin{pmatrix} A_{cl} & B_{cl} \\ C_{cl} & D_{cl} \\ I & 0 \\ 0 & I \end{pmatrix} \prec 0 \tag{4.17a}$$

$$\left(\begin{array}{cc} \Delta & 0 \\ 0 & \Delta \\ \hline I & 0 \\ 0 & I \end{array}\right)^T \begin{pmatrix} Q_e & 0 \\ 0 & R_e \end{pmatrix} \left(\begin{array}{cc} \Delta & 0 \\ 0 & \Delta \\ \hline I & 0 \\ 0 & I \end{array}\right) \succ 0 \tag{4.17b}$$

are satisfied. The following theorem is the main idea of the controller design.

Theorem 4.2.1. *[7] The following statements are equivalent:*

1. *There exists a controller of the form 4.10 such that there exist matrices χ and $R_e = -Q_e \succ 0$ that satisfy*

$$\chi \succ 0, \begin{pmatrix} A_{cl} & B_{cl} \\ C_{cl} & D_{cl} \\ \mathrm{I} & 0 \\ 0 & \mathrm{I} \end{pmatrix}^T \begin{pmatrix} 0 & 0 & 0 & \chi & 0 & 0 \\ 0 & R_e & 0 & 0 & 0 & 0 \\ 0 & 0 & \gamma^{-1}I & 0 & 0 & 0 \\ \chi & 0 & 0 & 0 & 0 & 0 \\ 0 & 0 & 0 & 0 & Q_e & 0 \\ 0 & 0 & 0 & 0 & 0 & -\gamma I \end{pmatrix} \begin{pmatrix} A_{cl} & B_{cl} \\ C_{cl} & D_{cl} \\ \mathrm{I} & 0 \\ 0 & \mathrm{I} \end{pmatrix} \prec 0 \tag{4.18}$$

2. *There exist $X = X^T$, $Y = Y^T$, $Q = Q^T = -R$, $\widetilde{Q} = \widetilde{Q}^T = -\widetilde{R}$ and multipliers where*

satisfy the linear matrix inequalities

$$\Psi^T \left(\begin{array}{c} * \\ * \\ \hline * \\ * \\ \hline * \\ * \end{array}\right)^T \left(\begin{array}{cc|cc|cc} 0 & X & 0 & 0 & 0 & 0 \\ X & 0 & 0 & 0 & 0 & 0 \\ \hline 0 & 0 & Q & 0 & 0 & 0 \\ 0 & 0 & 0 & R & 0 & 0 \\ \hline 0 & 0 & 0 & 0 & -\gamma I & 0 \\ 0 & 0 & 0 & 0 & 0 & \gamma^{-1} I \end{array}\right) \left(\begin{array}{ccc} \mathrm{I} & 0 & 0 \\ A & B_1 & B_p \\ \hline 0 & \mathrm{I} & 0 \\ C_1 & D_{11} & D_{1p} \\ \hline 0 & 0 & \mathrm{I} \\ C_p & D_{p1} & D_{pp} \end{array}\right) \Psi \prec 0 \qquad (4.19)$$

$$\Phi^T \left(\begin{array}{c} * \\ * \\ \hline * \\ * \\ \hline * \\ * \end{array}\right)^T \left(\begin{array}{cc|cc|cc} 0 & Y & 0 & 0 & 0 & 0 \\ Y & 0 & 0 & 0 & 0 & 0 \\ \hline 0 & 0 & \widetilde{Q} & 0 & 0 & 0 \\ 0 & 0 & 0 & \widetilde{R} & 0 & 0 \\ \hline 0 & 0 & 0 & 0 & -\gamma^{-1} I & 0 \\ 0 & 0 & 0 & 0 & 0 & \gamma \end{array}\right) \left(\begin{array}{ccc} -A^T & -C_1^T & -C_p^T \\ \mathrm{I} & 0 & 0 \\ \hline -B_1^T & -D_{11}^T & -D_{p1}^T \\ 0 & \mathrm{I} & 0 \\ \hline -B_p^T & -D_{1p}^T & -D_{pp} \\ 0 & 0 & \mathrm{I} \end{array}\right) \Phi \succ 0 \quad (4.20)$$

$$\begin{pmatrix} Y & \mathrm{I} \\ \mathrm{I} & X \end{pmatrix} \succ 0 \qquad (4.21)$$

and

$$\begin{pmatrix} R & I \\ I & \widetilde{R} \end{pmatrix} \succ 0. \qquad (4.22)$$

Here,Φ and Ψ are orthonormal basis matrices of $(B_2^T D_{12}^T D_{p2}^T)$ and $(C_2 D_{21} D_{2p})$ respectively.

Orthonormal basis matrix of M is denoted by $M_\perp$ or $ker(M)$ and it satisfy two conditions.

1. $M^T M_\perp = 0$
2. $[M M_\perp]$ is square and invertible.

Remark: Solving for the controller

After finding the multipliers and the Lyapunov matrix constructing the controller K depends on the 4.18. This inequality can be written as

$$\begin{pmatrix} A + BKC \\ I \end{pmatrix}^T \Omega \begin{pmatrix} A + BKC \\ I \end{pmatrix} < 0 \tag{4.23}$$

where

$$A := \begin{pmatrix} A^a & \widetilde{B}_1^a \\ \widetilde{C}_1^a & \widetilde{D}_{11}^a \end{pmatrix}, \; B := \begin{pmatrix} B_2^a \\ \widetilde{D}_{12}^a \end{pmatrix}, \; C := \begin{pmatrix} C_2^a & D_{21}^a \end{pmatrix} \tag{4.24}$$

The inequality 4.23 can be rewritten as

$$\begin{pmatrix} I \\ KC \end{pmatrix}^T \underbrace{\begin{pmatrix} A & B \\ I & 0 \end{pmatrix}^T \Omega \begin{pmatrix} A & B \\ I & 0 \end{pmatrix}}_{\Pi} \begin{pmatrix} I \\ KC \end{pmatrix} \prec 0 \tag{4.25}$$

Assume that Π has no zero eigenvalue then one can apply the Lemma C.0.1 to the inequality 4.25 and the following inequality can be achieved. This application is performed to take K outer part of the inequality.

$$\begin{pmatrix} -C^T K^T \\ I \end{pmatrix}^T \Pi^{-1} \begin{pmatrix} -C^T K^T \\ I \end{pmatrix} \succ 0 \tag{4.26}$$

The inequality 4.26 can be rewritten again as

$$\begin{pmatrix} K^T \\ I \end{pmatrix}^T \underbrace{\begin{pmatrix} -C^T & 0 \\ 0 & I \end{pmatrix}^T \Pi^{-1} \begin{pmatrix} -C^T & 0 \\ 0 & I \end{pmatrix}}_{\Gamma} \begin{pmatrix} K^T \\ I \end{pmatrix} \succ 0 \tag{4.27}$$

$V = \begin{pmatrix} V_{+1} \\ V_{+2} \end{pmatrix}$ is the eigenvector of the positive eigenvalues. The following equation can be written by taking V as a basis

$$\begin{pmatrix} V_{+1} \\ V_{+2} \end{pmatrix}^T \Gamma \begin{pmatrix} V_{+1} \\ V_{+2} \end{pmatrix} \succ 0 \tag{4.28}$$

Pre- and post-multiply by V_{+2}^{-T} and V_{+2}^{-1} gives

$$\begin{pmatrix} V_{+1}V_{+2}^{-1} \\ I \end{pmatrix}^T \Gamma \begin{pmatrix} V_{+1}V_{+2}^{-1} \\ I \end{pmatrix} \succ 0 \tag{4.29}$$

This shows that

$$K^T = V_{+1}V_{+2}^{-1} \tag{4.30}$$

5. LPV Control Design for the TRMS System

In this chapter, the LPV controller for the TRMS will be designed. Firstly the LFT representation of the TRMS is derived by the LFR Toolbox. Secondly, the system is developed with the weights and the filters and linearized model is obtained. Theorem 4.2.1 is the main part of the controller design. For that purpose, the inequalities (4.21), (4.19), (4.20) are solved to find the variables $X, Y, Q, R, \widetilde{Q}, \widetilde{R}$ and γ by the help of the YALMIP Toolbox and solver SeDuMi. Finally, controller is designed. The details are given in the following sections.

5.1. LFT Representation of the TRMS

The LFT representation is obtained by the help of LFR Toolbox. LFR Toolbox is developed by J.F. Magni. The toolbox considers modeling, manipulation, order reduction and approximation of uncertain systems in LFT form. It also contains Simulink patch for simulation of LFT form systems. The toolbox and more information is available in reference [8]. The procedure to obtain the LFT representation of TRMS by LFR Toolbox is given in detail.

The first step is to define the parameters of the system. The function `lfrs` is used for this purpose.

The parameters are defined to the toolbox as, `av` is a_v, `cosav` is $\cos(av)$, `sinav` is $\sin(av)$, `zdotah` is $\dot{a}_h$ and `zdotav` is $\dot{a}_v$. The purpose `zdotah` and `zdotav` is to put the parameters in the order that we indicated before. LFR toolbox construct the Δ block in the alphabetic order of the parameters.

The system matrices $A(p), B(p), C, D$ which are indicated in equation (2.39) are defined as `An,Bn,Cn,Dn` by putting the defined parameters `av`, `cosav`, `sinav`, `zdotah` and `zdotav` into the equation. To get the true solution, one have to pay attention while writing the equations. The equations should be in the form of *constants* × *parameters*, *e.g.,*

$$\underbrace{(km/(Jh \times Tv))}_{constant} \times \underbrace{cosav}_{parameter} .$$

Otherwise, the variation of the parameter is taken as the multiplication of the constant by the toolbox.

So far, the variation of the parameters are not defined. As default configuration, bounds of the each parameters are taken as $[-1,+1]$ by the toolbox. There are many different ways to normalize the system in the toolbox. However, we use the most user friendly way. The definition of the bounds of the parameters and the normalization of the system can be achieved by the function `[An,Bn,Cn,Dn]=normalizelfr([An,Bn, Cn,Dn],parname,dmin,dmax)`.

The inputs of the function are parameter dependent matrices, two row vectors which contains the maximum and the minimum values of the parameters and the string array which contains the name and the order of the parameters.

The unnecessary large bounds for the parameters can affect the performance of the controller. For that purpose, we try to compress the bounds as much as possible and obtained the following results.

	a_v	$\cos(a_v)$	$\sin(a_v)$	$\dot{a}_h$	$\dot{a}_v$
max	$\pi/1.5$	1	1	1	1
min	$-\pi/8$	-0.5	-0.5	-1	-1

After normalization, input-output LFR of the system is obtained by the function `abcd2lfr` which is called as `sysmin=abcd2lfr([An,Bn,Cn,Dn],6);`.

The inputs of the the function are the parameter dependent matrices and the state number of the system. The output `sysmin` is defined as lfr object in the Workspace of the

MATLAB. The matrices of nominal system and the Δ block is defined as follows

$$\begin{pmatrix} A & B_1 \\ C_1 & D_{11} \end{pmatrix} := \texttt{sysmin.a}, \begin{pmatrix} B_2 \\ D_{12} \end{pmatrix} := \texttt{sysmin.b}, \begin{pmatrix} C_2 & D_{21} \end{pmatrix} := \texttt{sysmin.c},$$

$D_{22} :=$ `sysmin.d` and $\Delta :=$ `sysmin.e`.

Finally, we obtained the Linear Fractional Representation of the TRMS system as illustrated in the figure 3.3.

5.2. Constructing the System

In this section, the construction of the objective system is presented. The schematic form of the system which we want to control, is represented in Figure 4.4. However, some details are not realized from the figure. As it is seen in Figure 5.1, low-pass filters and weights are added to the system. Low-pass filters allow only low frequency signals to pass. We used Butterworth low pass filter and passband edge frequency is chosen as $2\pi(rad/sec)$. The main objective is to make z_p (error) zero in steady state for given input. If we minimize the area of the output signals, we can increase the performance of the system. For that purpose, integrator operator can be used. However, in Laplace domain integrator operator is $\frac{1}{s}$ and that makes the system unstable. Therefore, we added positive term to satisfy the stability and finally obtained the weights as,

$$\begin{pmatrix} \frac{1}{s+1e^{-5}} & 0 \\ 0 & \frac{1}{s+1e^{-5}} \end{pmatrix}.$$

Reference [10] presents detail discussion about the importance of weights.

Although closed loop system can be derived by hand, MATLAB provides very useful function for that purpose called `linmod`. This function provides the state-space linear model of the system of ordinary differential equations described in the Simulink environment by specifying the input output channels. The Simlulink environment illustration of the system setup is presented in Figure 5.1 with denoted the channel names. This way, it can be seen that Figure 5.1 is the reflection of Figure 4.4.

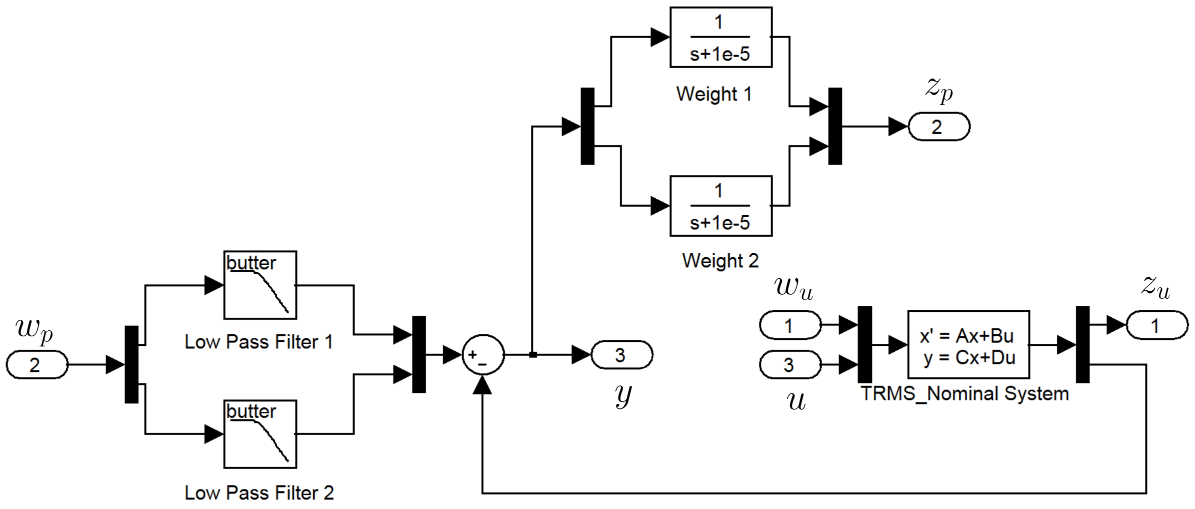

Figure 5.1. System Set-up

Consider the system equations (4.9) the structure of the output matrices AA, BB, CC and DD are defined as follows:

$$AA := A \tag{5.1}$$

$$BB := \begin{pmatrix} B_1 & B_p & B_2 \end{pmatrix} \tag{5.2}$$

$$CC := \begin{pmatrix} C_1 \\ C_p \\ C_2 \end{pmatrix} \tag{5.3}$$

$$DD := \begin{pmatrix} D_{11} & D_{1p} & D_{12} \\ D_{p1} & D_{pp} & D_{p2} \\ D_{21} & D_{2p} & D_{22} \end{pmatrix} \tag{5.4}$$

The corresponding MATLAB function is `[AA,BB,CC,DD]=linmod('systemsetup')`. This way, the system matrices are obtained. The next step is to construct the LMIs and find their solutions.

5.3. Constructing the LMIs

The this step is the construction of the LMIs. As mentioned in the beginning of this chapter. YALMIP Toolbox [11] provides functions for construction LMIs and SeDuMi [12] provides solver for the solution of the LMIs. The function `sdpvar` is used to construct the matrices. The decision variables $X, Y, Q, R, \widetilde{Q}, \widetilde{R}$ are constructed with this function. X, Y are $n \times n$ symmetric matrices. n is the amount of states. In this system n equals to 12. 6 states come from the model, two weights have 2 states and finally two second order low-pass filters give 4 states. X and Y defined by `X=sdpvar(n);` and `Y=sdpvar(n);`, respectively. The construction of the multipliers $Q, R, \widetilde{Q}, \widetilde{R}$ are more complicated than X, Y. The structure of the Q and $\widetilde{Q}$ depends Δ of the system to provide the inequality 4.8. The TRMS model has 5 parameters repeated 11 times, $\cos(a_v)$ repeated 5 times, $\sin(a_v)$ repeated 3 times, a_v,$\dot{a}_h$ and $\dot{a}_v$ repeated 1 time.

$$p_1 := a_v \tag{5.5}$$

$$p_2 := \cos(a_v) \tag{5.6}$$

$$p_3 := \sin(a_v) \tag{5.7}$$

$$p_4 := \dot{a}_h \tag{5.8}$$

$$p_5 := \dot{a}_v \tag{5.9}$$

and the structure of the Δ is

$$\Delta = \mathrm{diag}(p_1 I_1, p_2 I_5, p_3 I_3, p_4 I_1, p_5 I_1). \tag{5.10}$$

So the Q is defined as `Q1=sdpvar(1);`, `Q2=sdpvar(5);`, `Q3=sdpvar(3);`, `Q4=sdpvar(1);`, `Q5=sdpvar(1);`, `Q=blkdiag(Q1,Q2,Q3,Q4,Q5);` and `Q=-R`. The same procedure is applied for $\widetilde{Q}$ and $\widetilde{R}$. The value of $\gamma > 0$ is defined by user. The basis matrices Φ and Ψ is defined by the function called `null`.

After constructing the matrices, the set of the inequalities (4.21), (4.19) and (4.20) are developed. The function `set` is used for this purpose. The solution of the set of inequalities is obtained by the function `solvesdp`. Different solvers are developed for LMIs. LMILab is provided by MATLAB and it takes time to solve the inequality. Another solver called SeDuMi which can be obtained from [12] is used for solution. Although there is not a reasonable accuracy difference between solvers LMILab and SeDuMi, SeDuMi is much more faster than LMILab. As a notice, it should be mentioned that most of the time solvers give a solution but that does not mean the solution is valid for the desired condition. Because of this reason, one has to check the solution if it satisfy the desired conditions. The solution is found by trying the different values of the γ. For $\gamma = 2.73$, there is a solution for the system and the results are given for this value.

After finding the decision variables $X, Y, Q, R, \widetilde{Q}, \widetilde{R}$ and γ by solving the inequalities (4.21), (4.19) and (4.20), the next step is find the extension matrices Q_e, R_e and augmented matrices to develop the stability condition for closed loop.

The extension matrices are found as indicated in reference [7].

$$Q_e = \begin{pmatrix} Q & I \\ I & (Q - \widetilde{Q}^{-1})^{-1} \end{pmatrix} \text{ and } R_e = -Q_e. \tag{5.11}$$

The augmented matrices are developed as indicated in the equation (4.12). The controller is obtained by following the procedure that is indicated in the Remark part of the previous chapter.

Controller matrices which is defined in equation (4.10) are obtained by simple calculation. Because size of the controller matrices are big, we did not put it here. However the dimensions of the matrices can be summarized as $A_K^{12\times12}$, $B_{K_1}^{12\times11}$, $B_{K_2}^{12\times2}$, $C_{K_1}^{11\times12}$, $C_{K_2}^{2\times12}$, $D_{K_{11}}^{11\times11}$, $D_{K_{12}}^{11\times2}$, $D_{K_{21}}^{2\times11}$ and $D_{K_{22}}^{2\times2}$.

5.4. Simulation

The simulation is performed in Simulink environment. Designed controller is connected to non-linear model of TRMS. The framework is illustrated in Figure 5.2.

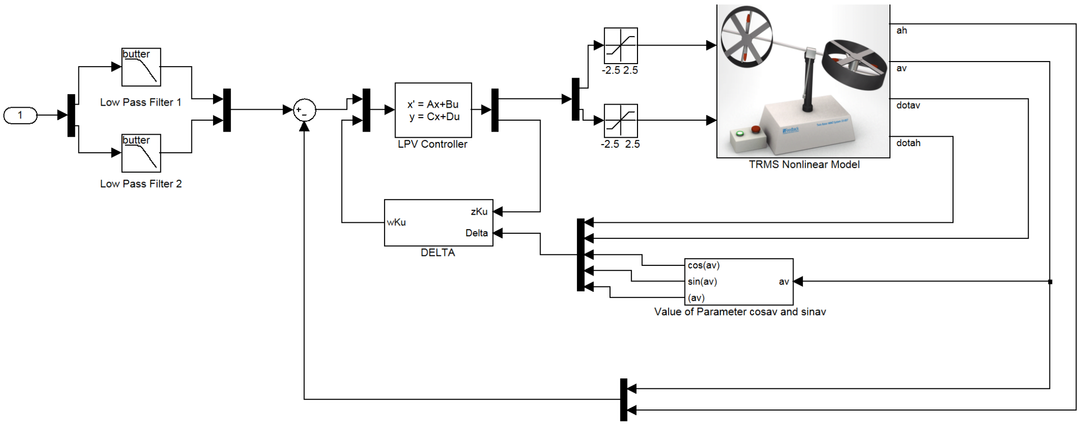

Figure 5.2. Simulation Framework in Simulink

In simulation part, one have to take the real life condition into consideration. Although controller works well in simulation, input of model may exceed the real life condition of system. The input of non-linear system of TRMS is voltage and in real life the value of the input voltage is bounded with physical condition. The physical bounds of D.C. motors of TRMS is $[-2.5, 2.5]$. To achieve the real life conditions, we use `saturation` block before inputs of nonlinear TRMS model.

We took successful results for several different conditions. Some simulation results are presented in the next chapter.

6. Simulation Results

In this chapter, we present simulation results of controlled nonlinear TRMS model for nine different modes. We consider all possible conditions. The detail of the modes are listed in Table 6.1. Each mode applied for one simulation. They are listed in order of difficulty. Firstly, step input is applied to the system for different orders. Secondly, sinusoidal and square wave signal are given as input. Finally, we observe the response of the system for different characteristics inputs. Consider the last two modes: Although TRMS is a coupled system, different desired conditions for each angle can be satisfied at the same time. As it can be seen from the results, designed controller works well for different modes.

The simulation results of the PID controller which is provided by Feedback Instruments Limited for mode 1 is presented in Figures 6.2(a) and 6.2(b). For pitch angle, *quasi*-LPV controller provides better overshoot than PID controller and settling times are very close. On the other hand, for yaw angle, the settling time of the simulation with *quasi*-LPV controller better than PID controller and the overshoots are close to each other.

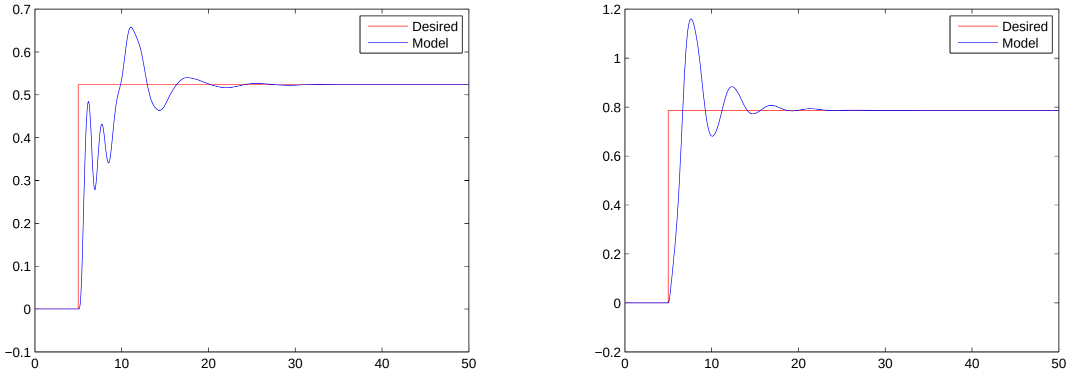

(a) Pitch Angle (Mode 1)

(b) Yaw Angle (Mode 1)

Figure 6.1. The Simulation Results of Angles (Mode 1)

Table 6.1. Characteristics of the sets of inputs

		Type	Frequency(rad/sec) - Step Time(sec)	Amplitude(rad)
Mode 1	Pitch	Step	5	$\pi/6$
	Yaw	Step	5	$\pi/4$
Mode 2	Pitch	Step	15	$\pi/6$
	Yaw	Step	5	$\pi/4$
Mode 3	Pitch	Step	5	$\pi/6$
	Yaw	Step	15	$\pi/4$
Mode 4	Pitch	Square	0.05π	$\pi/8$
	Yaw	Square	0.05π	$\pi/8$
Mode 5	Pitch	Square	0.1π	$\pi/8$
	Yaw	Square	0.05π	$\pi/8$
Mode 6	Pitch	Square	0.05π	$\pi/8$
	Yaw	Square	0.1π	$\pi/8$
Mode 7	Pitch	Sine	0.05π	$\pi/8$
	Yaw	Sine	0.1π	$\pi/8$
Mode 8	Pitch	Square	0.05π	$\pi/8$
	Yaw	Sine	0.1π	$\pi/8$
Mode 9	Pitch	Sine	0.1π	$\pi/8$
	Yaw	Square	0.05π	$\pi/8$

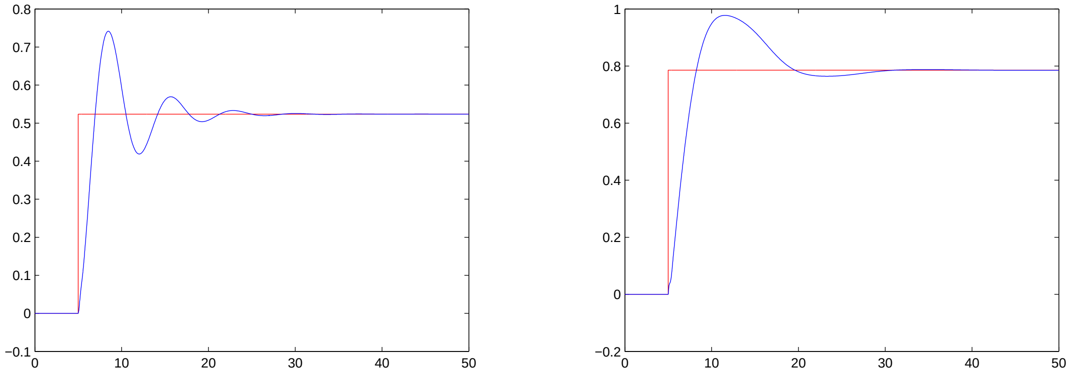

(a) The Simulation Result of PID Controller for Pitch Angle (Mode 1)

(b) The Simulation Result of PID Controller for Yaw Angle (Mode 1)

Figure 6.2. Simulation Results for PID Controller (Mode 1)

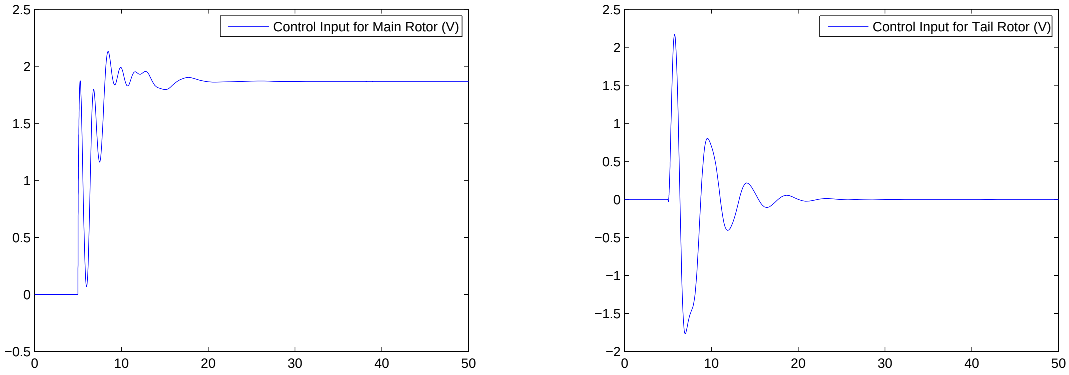

(a) Control input for Main Rotor (Mode 1)

(b) Control input for Tail Rotor (Mode 1)

Figure 6.3. Simulation Results of Control Input (Mode 1)

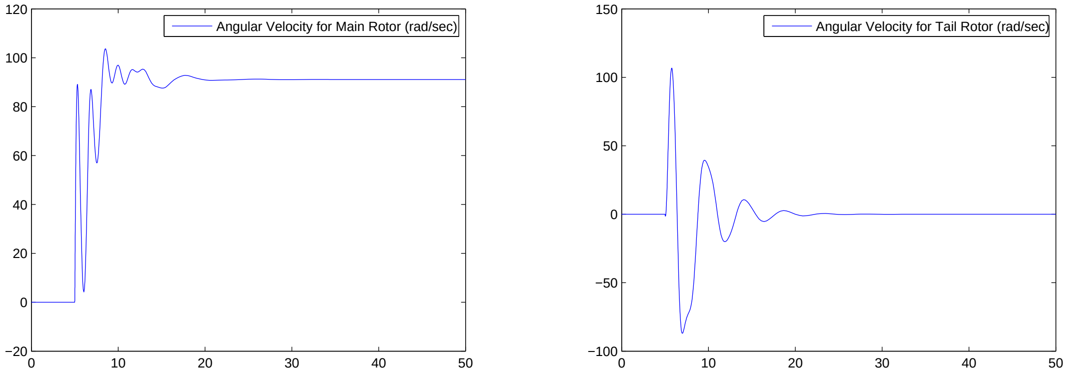

(a) Angular Velocity of Main Rotor (Mode 1)

(b) Angular Velocity of Tail Rotor (Mode 1)

Figure 6.4. Simulation Results of Angular Velocities (Mode 1)

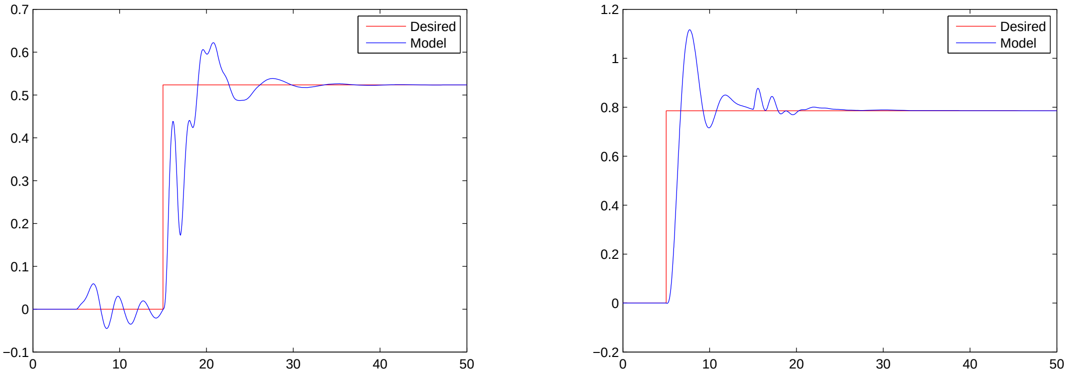

(a) Pitch Angle (Mode 2

(b) Yaw Angle (Mode 2

Figure 6.5. Simulation Results of Angles (Mode 2)

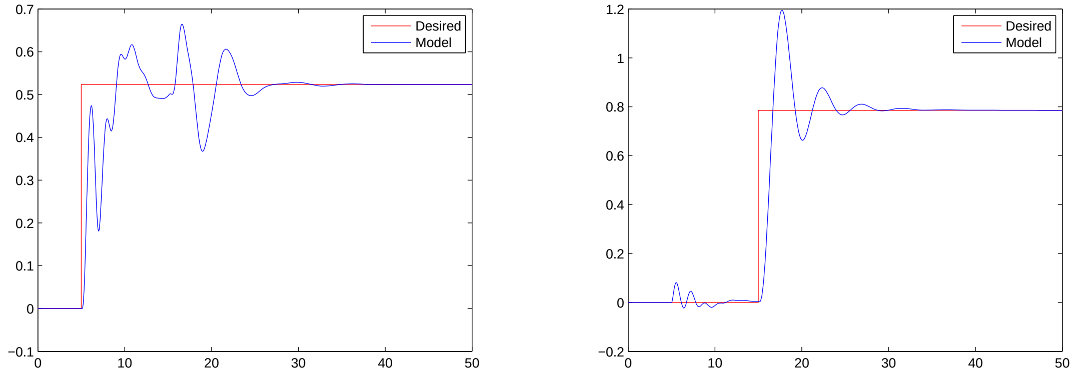

(a) Pitch Angle (Mode 3)

(b) Yaw Angle (Mode 3)

Figure 6.6. Simulation Results of Angles (Mode 3)

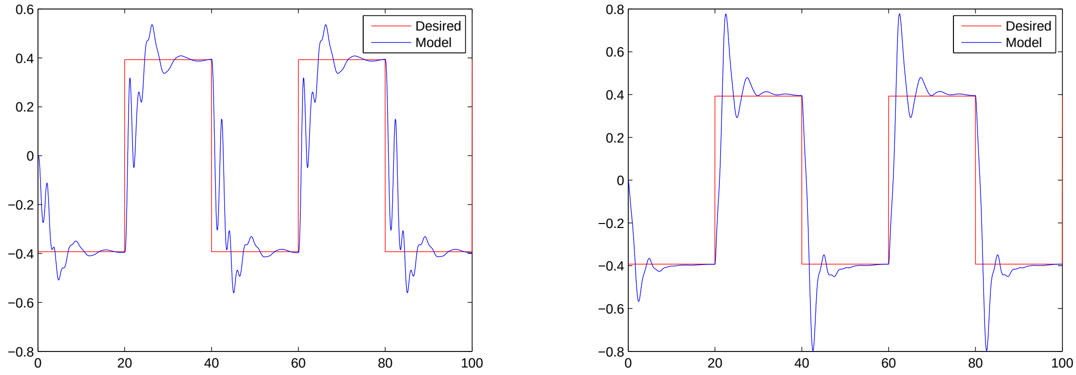

(a) Pitch Angle (Mode 4)

(b) Yaw Angle (Mode 4)

Figure 6.7. Simulation Results of Angles (Mode 4)

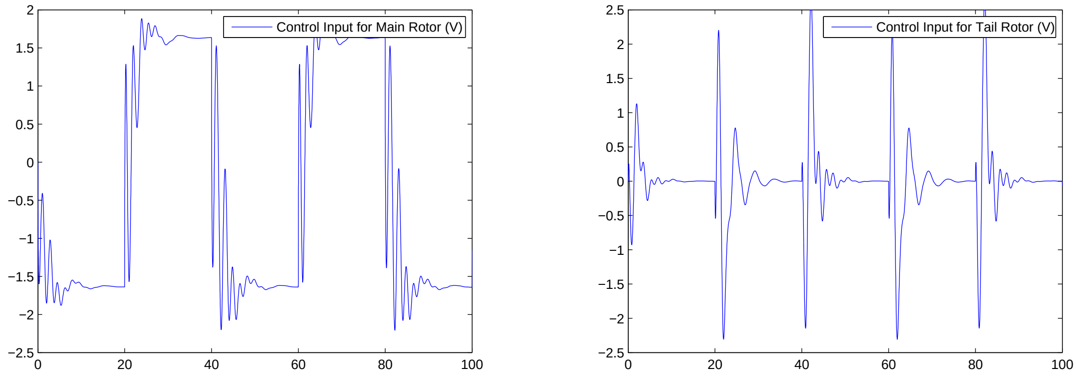

(a) Control input for Main Rotor (Mode 4) (b) Control input for Tail Rotor (Mode 4)

Figure 6.8. Simulation Results for Control Inputs (Mode 4)

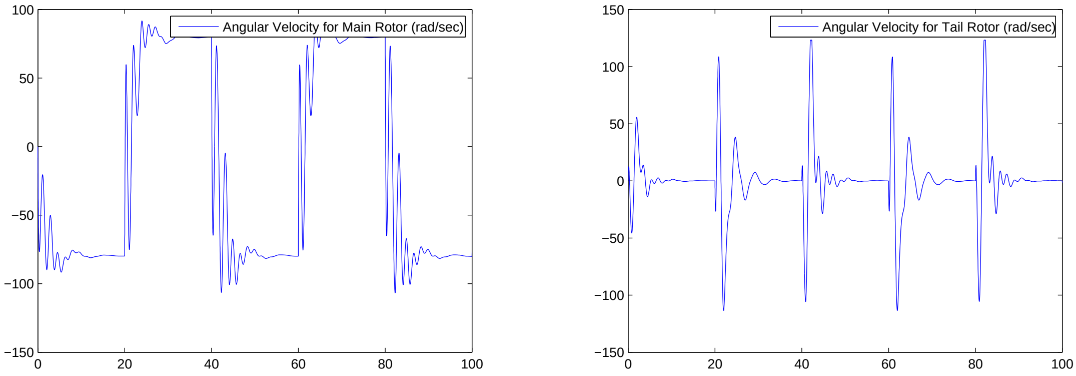

(a) Angular Velocity of Main Rotor (Mode 4) (b) Angular Velocity of Tail Rotor (Mode 4)

Figure 6.9. Simulation Result for Angular Velocity (Mode 4)

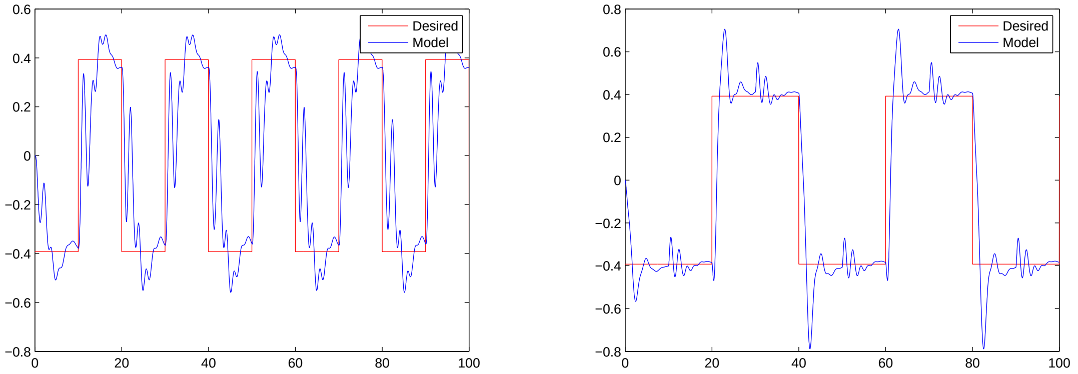

(a) Pitch Angle (Mode 5)

(b) Yaw Angle (Mode 5)

Figure 6.10. Simulation Result for Angles (Mode 5)

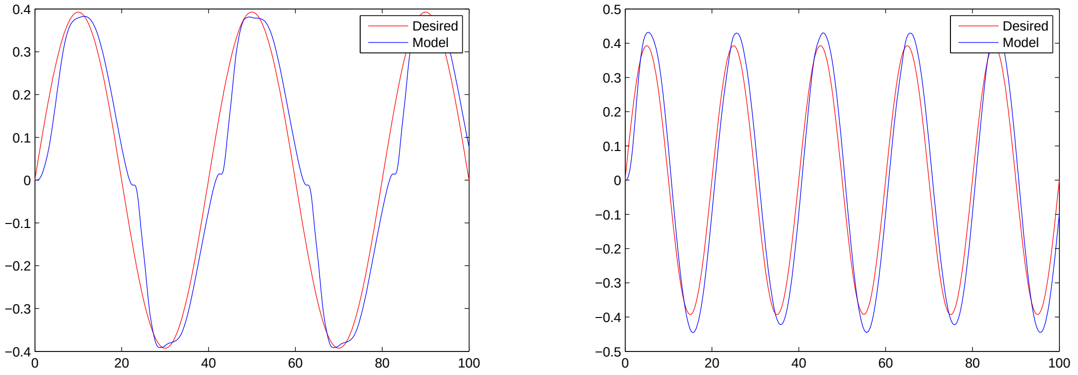

(a) Pitch Angle (Mode 7)

(b) Yaw Angle (Mode 7)

Figure 6.11. Simulation Result for Angles (Mode 7)

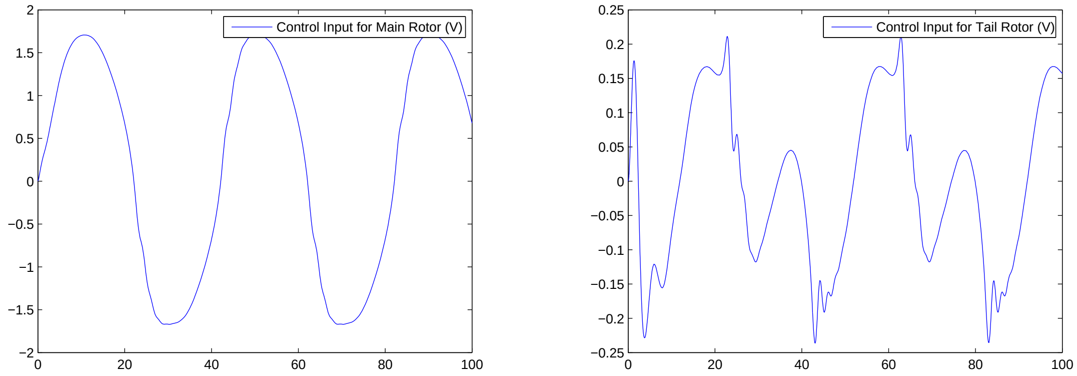

(a) Control Input for Mail Rotor (Mode 7)

(b) Control input for Tail Rotor (Mode 7)

Figure 6.12. Simulation Result for Control Input (Mode 7)

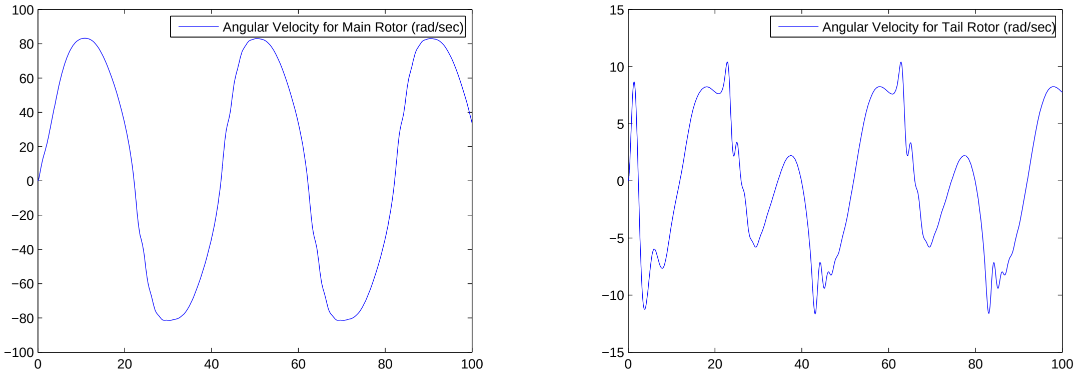

(a) Angular Velocity of Main Rotor (Mode 7)

(b) Angular Velocity of Tail Rotor (Mode 7)

Figure 6.13. Simulation Results for Angular Velocity (Mode 7)

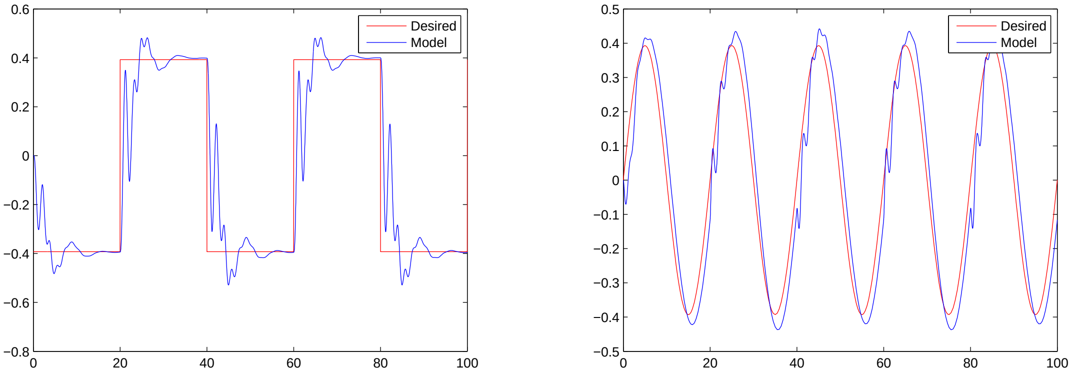

(a) Pitch Angle (Mode 8)

(b) Yaw Angle (Mode 8)

Figure 6.14. Simulation Result for Angles (Mode 8)

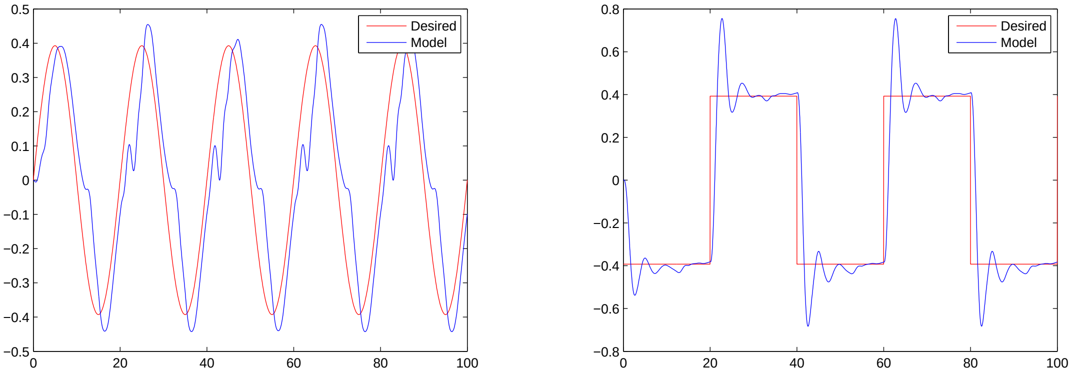

(a) Pitch Angle (Mode 9)

(b) Yaw Angle (Mode 9)

Figure 6.15. Simulation Result for Angles (Mode 9)

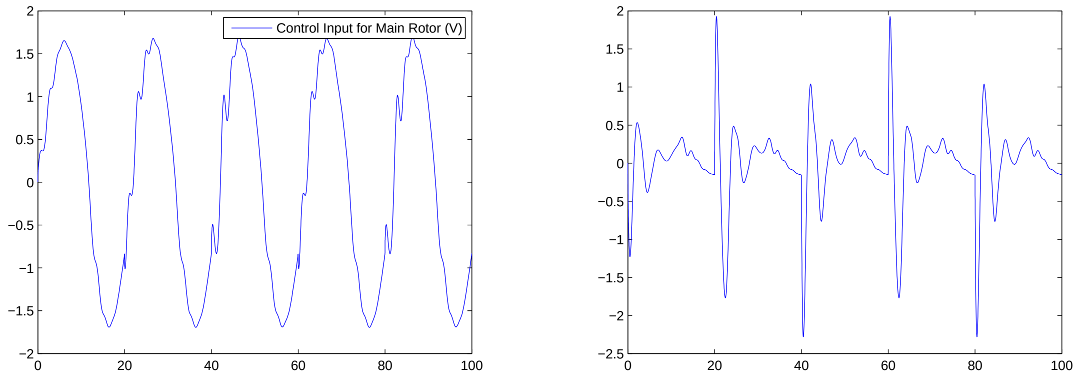

(a) Control input for Main Rotor (Mode 9)

(b) Control input for Tail Rotor (Mode 9)

Figure 6.16. Simulation Result for Control Inputs (Mode 9)

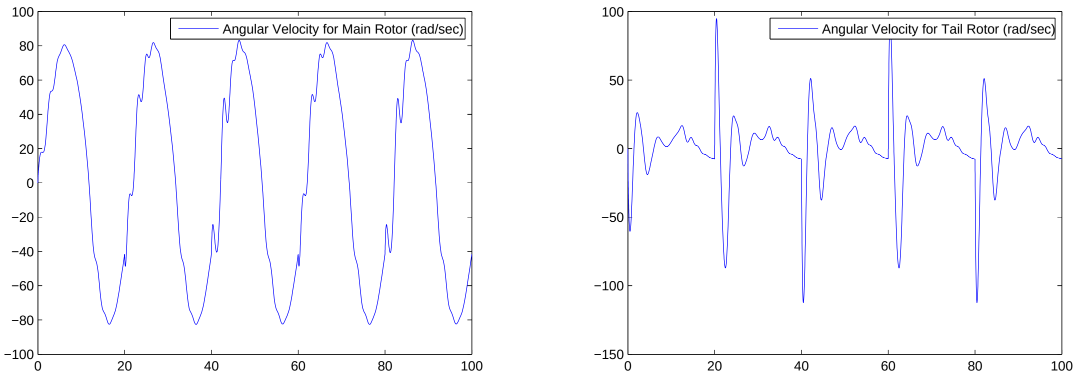

(a) Angular Velocity of Main Rotor (Mode 9)

(b) Angular Velocity of Tail Rotor (Mode 9)

Figure 6.17. Simulation Result for Angular Velocity (Mode 9)

7. CONCLUSIONS

In this thesis, we have investigated the use of LPV controller design for highly nonlinear and cross coupled TRMS. *Quasi*-LPV model of the system is developed by considering the nonlinearities in the mathematical model of the system as time varying parameters and the system is written as LFT form. LMI conditions for the existence of the controller and stability of the desired closed loop system are developed using LFT form of the system. Objective LPV controller for TRMS is reached solving the LMIs.

It is seen that simulation of designed LPV controller with nonlinear model of TRMS gives successful results for different modes.

LPV modeling and control has an important place in the literature. Several researches and investigations are made to improve the theory and obtain better results. In this thesis, it is showed that highly nonlinear system can be considered as an LPV system. In this way, developed LPV theory can be applied to reach an LPV controller to control the nonlinear model of the system.

APPENDIX A: Moment of Inertia of TRMS

The moment of inertias about vertical and horizontal axis are the sum of the all inertias. These can be calculated as:

The moment of inertia about horizontal axis J_v equals to

$$J_v = J_{mr} + J_m + J_{cb} + J_b + J_{tr} + J_t + J_{ms} + J_{ts} \tag{A.1}$$

where

$$\begin{aligned} J_{mr} &= m_{mr} l_m^2 && \text{(A.2)} \\ J_m &= m_m \frac{l_m^2}{3} && \text{(A.3)} \\ J_{cb} &= m_{cb} l_{cb}^2 && \text{(A.4)} \\ J_b &= m_b \frac{l_b^2}{3} && \text{(A.5)} \\ J_{tr} &= m_{tr} l_{tr}^2 && \text{(A.6)} \\ J_t &= m_t \frac{l_t^2}{3} && \text{(A.7)} \\ J_{ms} &= m_{ms} \frac{r_{ms}^2}{2} + m_{ms} l_{ms}^2 && \text{(A.8)} \\ J_{ts} &= m_{ts} r_{ts}^2 + m_{ts} l_t^2 && \text{(A.9)} \end{aligned}$$

and the moment of inertia about vertical axis J_h equals to

$$J_h = J_{h1} + J_{h2} + J_{h3} + J_{h4} + J_{h5} + J_{h6} + J_{h7} + J_{h8} \tag{A.10}$$

where

$$J_{h1} = m_m \frac{(l_m \cos(a_v))^2}{3} \tag{A.11}$$

$$\begin{aligned}
J_{h2} &= m_t \frac{(l_t \cos(a_v))^2}{3} && \text{(A.12)}\\
J_{h3} &= m_b \frac{(l_b \sin(a_v))^2}{3} && \text{(A.13)}\\
J_{h4} &= m_{tr}(l_t \cos(a_v))^2 && \text{(A.14)}\\
J_{h5} &= m_{mr}(l_m \cos(a_v))^2 && \text{(A.15)}\\
J_{h6} &= m_{cb}(l_{cb} \sin(a_v))^2 && \text{(A.16)}\\
J_{h7} &= m_{ts}\frac{r_{ts}^2}{2} + m_{ts}(l_t \cos(a_v))^2 && \text{(A.17)}\\
J_{h8} &= m_{ms}r_{ms}^2 + m_{ms}(l_m \cos(a_v))^2 && \text{(A.18)}
\end{aligned}$$

or in compact form

$$J_h = D\cos^2(av) + E\sin^2(a_v) + F \tag{A.19}$$

where

$$D = (\frac{m_m}{3} + m_{mr} + m_{ms})l_m^2 + (\frac{m_t}{3} + m_{tr} + m_{ts})l_t^2 \tag{A.20}$$

$$E = m_b\frac{l_b^2}{3} + m_{cb}l_{cb}^2,\ F = m_{ms}r_{ms}^2 + m_{ts}\frac{r_{ts}^2}{2} \tag{A.21}$$

APPENDIX B: Constants in Mathematical Model of TRMS

Constant Parameters	Value	Constant Parameter	Value
$l_t(m)$	0.282	$m_{ms}(kg)$	0.219
$l_m(m)$	0.246	$\widetilde{k}_{pv}$	1.62e-3
$l_b(m)$	0.290	$\widetilde{k}_{ph}$	1.84e-3
$l_{cb}(m)$	0.276	k_{pv}	1.62e-6
$r_{ms}(m)$	0.155	k_{ph}	1.84e-6
$r_{ts}(m)$	0.100	k_{fv}	5.45e-3
$m_{tr}(kg)$	0.221	k_{fh}	9.50e-3
$m_{mr}(kg)$	0.236	k_t	2.60e-5
$m_{cb}(kg)$	0.068	k_m	2.00e-4
$m_t(kg)$	0.015	T_v	5.22e-2
$m_m(kg)$	0.014	T_h	9.23e-3
$m_b(kg)$	0.022	K_v	1.08e-3
$m_{ts}(kg)$	0.119	K_h	1.98e-4

APPENDIX C: Auxiliary Lemma

The inertia of a matrix A is defined as $in(A) = (n_+, n_-, n_0)$ where

$$
\begin{aligned}
n_+ &:= \text{Number of the positive eigenvalues of } A \\
n_- &:= \text{Number of the positive eigenvalues of } A \\
n_0 &:= \text{Number of the zero eigenvalues of } A
\end{aligned}
$$

Lemma C.0.1. *[9] Let $\Pi = \Pi^T \in R^{(p+m)\times(p+m)}$ have $in(\Pi) = (p, m, 0)$ and let $K \in R^{m\times p}$ be given. Then,*

$$
\begin{pmatrix} I_m \\ K \end{pmatrix}^T \Pi \begin{pmatrix} I_m \\ K \end{pmatrix}^T \prec 0
$$

if and only if

$$
\begin{pmatrix} -K^T \\ I_p \end{pmatrix}^T \Pi^{-1} \begin{pmatrix} -K^T \\ I_p \end{pmatrix} \succ 0
$$

REFERENCES

1. *Twin Rotor MIMO System 33-20 User Manual*, 2005, Feedback Instruments Limited, Crowborough, UK.

2. Ahmed, S. *et al.*, 2000, “Dynamic Modeling and Optimal Control of a Twin Rotor MIMO System ”. *IEEE National Aerospace and Electronics Conference*,pp.391-398.

3. Shaheed, M. H., 2004, “Performance Analysis of Types of Conjugate Gradient Algorithm in the Non Linear dynamic Modeling of a TRMS Using Feedforward Neural Networks ”, *IEEE International Conference on Systems*,pp.5985-5990.

4. Aldebrez, F.M., I. Z. Mat Darus and M. O. Tokhi, 2004, “Dynamic Modeling of a Twin Rotor system in Hovering Position ”,*Symposium on Control, Comunications and Signal Processing*,pp.823-826.

5. Shaheed, M. H. and A. Rahideh, 2006, “Mathematical Dynamic Modeling of a Twin-Rotor Multiltiple Input-Multiple Output System” *Journal of Systems and Control Enginerring*, Vol. 221, pp. 2998-3008.

6. Boyd, S.P.*et. al.*, 1987, *Linear Matrix Inequalities in System and Control Theory*, SIAM, New Jersey.

7. Schere, C. W. and S. Wiland, *Lecture Notes: Linear Matrix Inequalities in Control*,http://www.dcsc.tudelft.nl/ cscherer/2416/lmi.html.

8. Magni, J. F., *Technical Report of Linear Fractional Represntation Toolbox, Modeling, Order Reduction, Gain Scheduling*, http://www.cert.fr/dcsd/idco/perso/Magni/msimulink/index.html.

9. Köse, İ. E, 2002, “IQC-Based L2 Control of Linear Periodic Sytems”,*Systems and control Letters*, Vol. 47, pp. 199-109.

10. Zhou, K., J. C. Doyle and K. Glover, 2002, *Robust and Optimal Control*, Prentice-Hall, New Jersey.

11. Löfberg, J., *YALMIP Toolbox* http://control.ee.ethz.ch/ joloef/yalmip.php

12. AOL Research Group in McMaster University, *SeDuMi Solver* http://sedumi.mcmaster.ca/component

13. *System Dynamcis*, http://www.tmt.ugal.ro/crios/Support/ANPT/Curs/sdyn